UNIVERSIDADE ESTADUAL DE MARINGÁ
CENTRO DE CIÊNCIAS AGRÁRIAS
Programa de Pós-Graduação em Ciência de Alimentos

FILTRAÇÃO POR MEMBRANAS NO PROCESSAMENTO DE EXTRATO DE HIBISCO (*Hibiscus sabdariffa* L.)

CAROLINA MOSER PARAÍSO

Maringá
2021

CAROLINA MOSER PARAÍSO

FILTRAÇÃO POR MEMBRANAS NO PROCESSAMENTO DE EXTRATO DE HIBISCO (*Hibiscus sabdariffa* L.)

Tese apresentada ao programa de pós-graduação em Ciência de Alimentos da Universidade Estadual de Maringá, como parte dos requisitos para obtenção do título de doutor em Ciência de Alimentos

Maringá
2021

Dados Internacionais de Catalogação-na-Publicação (CIP)
(Biblioteca Central - UEM, Maringá - PR, Brasil)

Paraíso, Carolina Moser
P222f Filtração por membranas no processamento de extrato de hibisco (Hibiscus sabdariffa L.) / Carolina Moser Paraíso. -- Maringá, PR, 2021.
93 f.color., figs., tabs.

Orientadora: Profa. Dra. Grasiele Scaramal Madrona.
Tese (Doutorado) - Universidade Estadual de Maringá, Centro de Ciências Agrárias, Departamento de Ciências Agronômicas, Programa de Pós-Graduação em Ciência de Alimentos, 2021.

1. Membranas - Filtração. 2. Antioxidante. 3. Incrustação. 4. Hibiscus sabdariffa L. 5. Compostos fenólicos. I. Madrona, Grasiele Scaramal, orient. II. Universidade Estadual de Maringá. Centro de Ciências Agrárias. Departamento de Ciências Agronômicas. Programa de Pós-Graduação em Ciência de Alimentos. III. Título.

CDD 23.ed. 660.284245

Rosana de Souza Costa de Oliveira - 9/1366

CAROLINA MOSER PARAÍSO

"FILTRAÇÃO POR MEMBRANAS NO PROCESSAMENTO DE EXTRATO DE HIBISCO (HIBISCUS SABDARIFFA L.)"

Tese apresentada à Universidade Estadual de Maringá, como parte das exigências do Programa de Pós-graduação em Ciência de Alimentos, para obtenção do grau de Doutor em Ciência de Alimentos.

Aline J. C. Baptista

Profa. Dra. Aline Takaoka Alves Baptista

Prof. Dr. Carlos Eduardo Barão

Camila S. Mangolim

Profa. Dra. Camila Sampaio Mangolim

Rúbia C. G. Corrêa

Prof. Dra. Rúbia Carvalho Gomes Corrêa

Madrona

Profa. Dra. Grasiele Scaramal Madrona
Orientadora

Maringá – 2021

Orientadora
Grasiele Scaramal Madrona

BIOGRAFIA

Carolina Moser Paraíso nasceu em 03 de março de 1992 na cidade de Maringá, Paraná.

Possui graduação em Engenharia de Alimentos e mestrado em Ciência de Alimentos pela Universidade Estadual de Maringá (UEM).

Tem experiência nas áreas de tecnologia e ciência de alimentos, atuando principalmente nos seguintes temas: extração de compostos bioativos, filtração por membranas de extratos vegetais e análises antioxidantes.

Dedico

Aos meus pais, Paulo e Solange,

A minha vó Ondina,

que me apoiam sempre em todos os meus sonhos e objetivos.

AGRADECIMENTOS

A Deus, pela minha vida e por estar sempre guiando o meu caminho.

Aos meus pais Paulo e Solange, por confiar, torcer e sempre me incentivar pelo decorrer da minha vida.

A minha vó Ondina, por toda a ajuda, motivação e orações.

A minha tia Marcia e meu primo Gabriel por sempre estarem presentes e torcerem por mim.

Ao meu namorado Dalvan pelo companheirismo e apoio.

Aos colegas do grupo de pesquisa pelo conhecimento compartilhado e no desenvolvimento dos experimentos. Um agradecimento em especial para minha amiga e parceira de laboratório Suelen por me ajudar sempre na minha pesquisa.

A minha orientadora e amiga, professora Dra. Grasiele Scaramal Madrona, pela imensa confiança em mim depositada desde o início da graduação e pelo conhecimento compartilhado.

Aos professores Miria Hespanhol Miranda Reis, Jesuí V. Visentainer, Silvio Claudio da Costa e Francielle Sato pela parceria na disponibilização de laboratórios, equipamentos e o conhecimento para o desenvolvimento deste trabalho.

Ao técnico de laboratório Antônio Sérgio Dacome pela parceria e disposição em sempre me ajudar a montar os sistemas de filtração por membranas.

APRESENTAÇÃO

Esta dissertação está apresentada na forma de DOIS artigos científicos.

1. Carolina Moser Paraíso, Suelen Siqueira dos Santos, Lidiane Pereira Bessa, Ana Paula Lopes, Camilla Yara Langer Ogawa, Silvio Cláudio da Costa, Miria Hespanhol Miranda Reis, Ubirajara Coutinho Filho, Francielle Sato, Jesuí V. Visentainer, Grasiele Scaramal Madrona. Performance of asymmetric spinel hollow fiber membranes for hibiscus (*Hibiscus sabdariffa L.*) extract clarification: flux modeling and extract stability
Publicado na revista: Journal of Food Processing and Preservation
Qualis B1 em ciência de alimentos

2. Carolina Moser Paraíso, Jessica dos Santos Pizzo, Mariana Sversut Gibin, Eduardo Azzolini Volnistem, Jesuí V. Visentainer, Francielle Sato, Silvio Cláudio da Costa, Miria Hespanhol Miranda Reis, Grasiele Scaramal Madrona. Investigation of techniques to mitigate membrane fouling in cross-flow ultrafiltration of hibiscus (*Hibiscus sabdariffa L.*) extract
A submeter a revista: Food and Bioprocess Technology
Qualis A1 em ciência de alimentos.

GENERAL ABSTRACT

INTRODUCTION

Hibiscus sabdariffa L., also known as hibiscus or roselle, is a plant species of the *Malvaceae* family grown worldwide. The commercial interest of hibiscus is mainly in dry calyces that have in their composition high content of antioxidant molecules (anthocyanins, flavonoids, and phenolic acids) capable of reduce disease risks. Membrane filtration is a technique based on the permeation of solute molecules through a semipermeable membrane, being an efficient alternative for clarification and concentration of plant extracts, due to the preservation of product characteristics. This process offers several advantages, including low temperature operation, no phase transition, high separation efficiency, low power consumption, simple equipment and easy scale-up. The greatest limitation for membrane separation processes is membrane fouling, since during operation particles are deposited in the membrane (surface and/or pores). Therefore, it is essential to understand the mechanisms of membrane fouling and provide solutions for this problem.

AIMS

The general objective of this work was to apply membrane filtration processes to hibiscus *(Hibiscus Sabdariffa* L.) extracts. The specific objectives were: (1) To evaluate the application of centrifugation followed by membrane filtration to produce ready-to-drink tea with high antioxidant content and (2) To use turbulence promotor and ultrasound in filtration to reduce membrane fouling.

MATERIALS AND METHODS

This study is divided into two parts, in the first the focus was filtration through asymmetric hollow fiber membranes with composition of 25% dolomite and 75% alumina (pore sizes ranging from 0.16 to 5.29 μm) for the clarification of hibiscus extract with and without centrifugation (8000 rpm for 20 min). In the second part of the study, the use of 3D turbulence promoters (108 pins, spacing of 6 mm between pins, 2.5 mm in diameter and 1.8 mm in height), ultrasound (Ultracleaner 1650 Unique, frequency of 40 KHz) and the association of turbulence promoter plus ultrasound to mitigate fouling in flat membranes of polyethersulfone (5 kDa) during

cross-flow ultrafiltration of hibiscus extract. In the two stages of the study, hibiscus extracts and permeated extracts were analyzed for pH, total soluble solids, total solids, total phenolic compounds, total anthocyanins, antioxidant (DPPH and FRAP), instrumental color and chromatographic analysis (UPLC-MS/MS). Mathematical modeling and the resistance series model were performed to describe the scale during extract filtration. In the first part, tea cream was evaluated and membranes were characterized before and after filtration with scanning electron microscopy (MEV), and Fourier transform infrared spectroscopy (FTIR-ATR). In the second part, membranes were evaluated by atomic force microscopy (AFM) and Fourier transform infrared spectroscopy (FTIR-ATR). The data were statistically evaluated using variance analysis (ANOVA), and Tukey test with a significance level of 5% ($p \leq 0.05$) using the statistical program Sisvar 5.6.

RESULTS AND DISCUSSION

In the first part of the study it was observed that centrifugation provided a significant improvement in permeate flux in the asymmetric hollow fiber membrane. For extracts without centrifugation the initial flux was 460.23 kg m^{-2} h^{-1}, whereas for centrifuged extracts the initial flux was 694.79 kg m^{-2} h^{-1} representing a flux increase of 51%. Complete pore blockage (n=2) was the main fouling mechanism and according to SEM and FTIR-ATR data, polysaccharides, proteins and phenolic compounds were probably responsible for fouling. After sequential membrane filtration total soluble solids and total solids were reduced from 5.53 to 4.03 °Brix, and 47120 to 37780 mg L^{-1}, respectively. Clarification of the product also occurred after sequential membrane filtration, in which the L* color coordinate increased from 15.69 to 22.03. Seven compounds were identified by UPLC-MS/MS in the extracts and permeate: Cyanidine (m/z 287.1), delphinidin (m/z 303.1), 4-cafeoglycenquine acid (m/z 353 0), hexoside quercetin (m/z 463.0), quercetin (m/z 595.0), myricetin (m/z 611.0) and kaempferol (m/z 285.0). Centrifuged extracts with membrane filtration showed greater stability after 20 days of storage at 5°C, with 43.1% reduction in tea cream formation. In the second part of the study, it was observed that the use of ultrasound, turbulence promoter, and ultrasound plus turbulence promoter, increased the flux by 21, 44 and 88%, respectively. Pore blockage was the main fouling mechanism and polysaccharides, proteins and bioactive compounds probably caused membrane fouling as shown by FTIR-ATR results. AFM analysis exposed membrane roughness after filtration, and compared with the roughness of the virgin membrane, the control membrane was 12 times larger, while the membrane from ultrasound plus turbulence promoter was only 2 times larger. Retention greater than 60% was observed for total phenolic compounds, total anthocyanins, cyanidine-3-glycoside, delphinidin, quercetin, myricetin, and rutin after ultrafiltration.

CONCLUSION

Through this study, it was possible to conclude that:

- The application of centrifugation as pretreatment resulted in higher permeate fluxs in filtration by asymmetric hollow fiber membrane. Furthermore, it is important to highlight that the centrifuged and filtered extract was clarified and presented greater stability after 20 days of storage at 5°C, reducing the formation of tea cream. Thus, the sequential process of pretreatment (centrifugation) and membrane filtration can be potentially applied to produce ready-to-drink hibiscus tea, with high antioxidant content.

- The use of ultrasound, turbulence promoter, and ultrasound plus turbulence promoter, for membrane filtration resulted in higher fluxes of hibiscus extract permeate. Polysaccharides, proteins and bioactive compounds were most likely responsible for membrane fouling. Furthermore, it is important to highlight that the use of turbulence promoter in association with ultrasound did not alter the quality of hibiscus extract. Thus, the combined use of turbulence promoter and ultrasound in the ultrafiltration module shows great potential to significantly mitigate membrane fouling and improve cross-flow filtration.

Keywords: membrane, fouling, phenolic compounds, antioxidant.

RESUMO GERAL

INTRODUÇÃO

O *Hibiscus sabdariffa* L., também conhecido como hibisco ou roselle, é uma espécie vegetal da família *Malvaceae*, cultivado mundialmente. Seu interesse comercial está principalmente nos cálices secos que possuem em sua composição alto teor de moléculas com caráter antioxidante (antocianinas, flavonoides e ácidos fenólicos) capazes de reduzir o risco de doenças. O processo de filtração por membrana é uma técnica baseada na permeação do soluto através de uma membrana semipermeável, sendo uma alternativa eficiente para clarificação e concentração de extratos vegetais, devido à preservação das características do produto. Este processo oferece várias vantagens, incluindo uso de baixa temperatura, ausência de transição de fase, alta eficiência de separação, baixo consumo de energia, equipamento simples e fácil aumento de escala. A maior limitação para a utilização deste processo é a formação de incrustação, em que, durante a operação partículas são depositadas na membrana, sendo fundamental compreender os mecanismos de incrustação e fornecer o controle para tal problema.

OBJETIVOS

Este trabalho teve como objetivo aplicar o processo de filtração por membranas em extratos de cálices de hibisco. Como objetivos específicos: (1) Aplicação de centrifugação seguida de filtração por membranas para produzir chá pronto para beber, com alta capacidade antioxidante e (2) Utilizar promotor de turbulência e ultrassom na ultrafiltração visando a redução da incrustação na membrana.

MATERIAIS E MÉTODOS

Este trabalho está dividido em duas partes, sendo que a primeira o foco foi aplicação de filtrações através de membranas de fibras ocas assimétricas com composição de 25% dolomita e 75% de alumina (tamanhos de poros variando de 0,16 a 5,29 µm) para a clarificação do extrato de hibisco com e sem centrifugação (8000 rpm por 20 min) como pré tratamento. Na segunda parte do trabalho foi avaliado o uso de promotor de turbulência 3D (108 pinos, espaçamento de 6 mm entre os pinos, 2,5 mm de diâmetro interno e 1,8 mm de altura), ultrassom (Ultracleaner 1650 Unique, frequência de 40 KHz) e a associação do promotor de turbulência com ultrassom para mitigação da formação de incrustação em membranas planas de polietersulfona (5 kDa) durante ultrafiltrações *cross-flow* do extrato de hibisco. Nas duas etapas do trabalho, os extratos de hibisco e os permeados foram analisados quanto ao pH, total de sólidos solúveis, sólidos totais, compostos fenólicos totais, antocianinas totais, antioxidante (DPPH e FRAP), cor instrumental e análise cromatográfica (UPLC-MS/MS). Para avaliar/descrever a incrustação utilizou-se a modelagem matemática e o modelo de resistência em série durante a filtração. Na primeira etapa, avaliou-se o *tea cream* e as membranas foram caracterizadas antes e após a filtração com microscopia eletrônica de varredura (MEV), espectroscopia no infravermelho por transformada de Fourier (FTIR-ATR). Na segunda etapa avaliou-se as membranas por microscopia de força atômica (AFM) e espectroscopia no infravermelho por transformada de Fourier (FTIR-ATR). Os dados foram avaliados, por meio da Análise de Variância (ANOVA), e pelo teste de Tukey com significância de 5% ($p \leq 0{,}05$) utilizando o programa estatístico Sisvar 5.6.

RESULTADOS E DISCUSSÃO

Na primeira parte do trabalho foi observado que a centrifugação proporcionou uma melhora significativa no fluxo do permeado na membrana assimétrica de fibra oca, sendo que para o extrato sem centrifugação, o fluxo inicial foi de 460,23 kg m^{-2} h^{-1} e com a centrifugação o fluxo inicial foi de 694,79 kg m^{-2} h^{-1}, representando um aumento de fluxo de 51%. O bloqueio completo de poros (n=2) foi o principal mecanismo de incrustação do processo, sendo que de acordo com dados (SEM e FTIR-ATR), polissacarídeos, proteínas e compostos fenólicos que provavelmente foram os responsáveis pelo *fouling*. Após filtração sequencial por membrana, sólidos solúveis totais e sólidos totais foram reduzidos de 5,53 para 4,03 °Brix, 47120 para 37780 mg L^{-1}. Também ocorreu a clarificação do produto após a filtração sequencial por membrana, em que a coordena de cor L* aumentou de 15,69 para 22,03. Foram identificados sete compostos por UPLC-MS/MS nos extratos e permeados: Cianidina (m/z 287.1), delfinidina (m/z 303.1), ácido 4-cafeoilquínico (m/z 353.0), quercetina hexoside (m/z 463.0), quercetina (m/z 595.0), mirecetina (m/z 611.0) e kaempferol (m/z 285.0). O extrato centrifugado seguido de filtração por membrana apresentou maior estabilidade após 20 dias de armazenamento a

5°C, com redução no tea cream de 43,1%. Na segunda parte do trabalho foi observado que o uso de ultrassom, promotor de turbulência e a associação de ultrassom e promotor de turbulência, aumentaram o fluxo em 21, 44 e 88%, respectivamente. O bloqueio de poros foi o principal mecanismo de incrustação dos processos, sendo que polissacarídeos, proteínas e compostos bioativos que provavelmente causaram a incrustação na membrana como confirmado pelos resultados de FTIR-ATR. A análise de AFM mostrou que comparado com a rugosidade da membrana virgem, a membrana controle foi 12 vezes maior e a membrana com associação do promotor e ultrassom foi de somente 2 vezes. Uma retenção maior que 60% foi observada para compostos fenólicos totais, antocianinas totais, cianidina-3-glicosídeo, delfinidina, quercetina, mirecetina e rutina após a ultrafiltração.

CONCLUSÃO

Por meio deste trabalho foi possível concluir que:

- A aplicação da centrifugação como pré tratamento resultou em maiores fluxos de permeado na filtração por membrana assimétrica de fibra oca. Ainda, é importante destacar que o extrato centrifugado e filtrado foi clarificado e apresentou maior estabilidade após 20 dias de armazenamento a 5°C, reduzindo a formação de *tea cream*. Assim, o processo sequencial centrifugação/filtração através de membranas de fibras ocas assimétricas pode ser potencialmente aplicado para produzir chá prontos para beber de hibisco, com alta capacidade antioxidante.

- A aplicação do ultrassom, promotor de turbulência e a associação desses dois métodos para a filtração por membrana resultou em maiores fluxos de permeado de extrato de hibisco, sendo que polissacarídeos, proteínas e compostos bioativos foram provavelmente responsáveis pela incrustação. Ainda, é importante destacar que o uso de promotores de turbulência em associação com o ultrassom não alterou a qualidade do extrato de hibisco. Assim, a combinação do uso de promotor de turbulência e ultrassom no módulo de ultrafiltração mostra um grande potencial para mitigar significativamente a incrustação da membrana e melhorar o fluxo de filtração em fluxo cruzado.

Palavras-chave: membrana, incrustação, compostos fenólicos, antioxidante.

ARTIGO 1

Performance of asymmetric spinel hollow fiber membranes for hibiscus (*Hibiscus sabdariffa L.*) **extract clarification: flux modeling and extract stability**

Carolina Moser Paraíso[a*], Suelen Siqueira dos Santos[a], Lidiane Pereira Bessa[b], Ana Paula Lopes[e], Camilla Yara Langer Ogawa[c], Silvio Cláudio da Costa[d], Miria Hespanhol Miranda Reis[b], Ubirajara Coutinho Filho[b], Francielle Sato[c], Jesuí V. Visentainer[e], Grasiele Scaramal Madrona[f]

[a] Programa de Pós-graduação em Ciência de Alimentos, Universidade Estadual de Maringá, Avenida Colombo 5790, Maringá-PR, Brazil. *carolina.moser@hotmail.com

[b] Faculdade de Engenharia Química, Universidade Federal de Uberlândia, Av. João Naves de Ávila, 2121, Uberlândia-MG, Brazil

[c] Departamento de Física, Universidade Estadual de Maringá, Avenida Colombo 5790, Maringá-PR, Brazil.

[d] Departamento de Bioquímica, Universidade Estadual de Maringá, Avenida Colombo 5790, Maringá-PR, Brazil.

[e] Departamento de Química, Universidade Estadual de Maringá, Avenida Colombo 5790, Maringá-PR, Brazil.

[f] Departamento de Engenharia de Alimentos, Universidade Estadual de Maringá, Avenida Colombo 5790, Maringá-PR, Brazil.

Abstract

This work evaluates a filtration process with and without centrifugation through asymmetric spinel hollow membranes for clarification of hibiscus extract. The centrifugation step increased the steady state flux through the membrane in 23.4%. Complete pore blockage was the main fouling mechanism and polysaccharides, proteins and phenolic compounds were mostly responsible for fouling. After sequential membrane filtration, total soluble solids, total solids and L* color coordinate (luminosity) were reduced from 5.53 to 4.03 ^{0}Brix, 47120 to 37780 mg L^{-1}, and 15.69 to 22.03, respectively. Seven individual bioactive compounds were identified in both extract and permeate by ultra performance liquid chromatography - mass spectrometer. The filtrated extract showed greater stability than the feed extract after 20 storage days (reduction of 43.1**%** in tea cream formation). The sequential centrifugation and filtration through asymmetric spinel hollow membranes can be potentially applied to produce hibiscus ready-to-drink tea with high antioxidant content.

Keywords: Tea cream, antioxidant activity, centrifugation, flux modeling.

Practical Applications

Membrane separation process is a filtration technique based on the permeation of solute molecules through a semipermeable membrane. The ceramic membrane is widely used for the purification and clarification of food products, but the cost of material is a disadvantage for the use of filtration processes. This work demonstrated the possibility of exploring the use of asymmetric spinel hollow membrane in clarification and increased stability of teas ready for consumption. This membrane presents composition of 25 wt% of dolomite and 75 wt% of alumina, thus presenting high stability, high permeate fluxes and low-cost ceramic material. This filtration technology membrane can also be combined as a pre-treatment, such as centrifugation, thus improving filtration efficiency and product stability. Finally, the new membrane used was feasible to produce a hibiscus tea ready-to-drink rich in antioxidants.

1. Introduction

Hibiscus sabdariffa L., also known as roselle or hibiscus, is a medicinal shrub of the genus *Hibiscus* of the family *Malvaceae*, being grown mainly for the preparation of tea and beverages based on edible calyces. Hibiscus calyces are a potential source of bioactive molecules, such as phenolic compounds and anthocyanins, which exhibit multiple biological effects (Cid-Ortega & Guerrero-Beltrán, 2015; Da-costa-rocha, Bonnlaender, Sievers, Pischel, & Heinrich, 2014). Some studies have confirmed pharmacological properties of dry calyx extract, including prevention of hypertension, inflammation, liver issues, diabetes, metabolic syndrome, among others (Riaz & Chopra, 2018). The major components found in hibiscus calyxes are the delphinidin 3 -O-sambubioside and cyanidin 3-O-sambubioside anthocyanins, which are responsible for the plants red color (Sinela et al., 2017). The largest consumption of hibiscus occurs in the form of tea; however ready-to-drink tea may form tea cream during storage. Tea cream is the precipitation of tea solids that are formed under cooling as a result of polyphenol interaction with other tea constituents, such as metal cations, proteins, lipids and polysaccharides (Chandini, Rao, & Subramanian, 2013; Sousa, Cabral, Madrona, Cardoso, & Reis, 2016).

Membrane filtration and centrifugation technologies are alternatives for product clarification and prevention to tea cream formation, since some components responsible for molecule complexations are selectively removed (Bindes, Cardoso, Reis, & Boffito, 2019). Centrifugation is suggested to be used as pretreatment prior to membrane filtration, since primary extract clarification by centrifugation removes suspended solids and increases the efficiency of sequential filtration (Bindes et al., 2019). There are few reports in the literature about stabilization of hibiscus extract by membrane filtration. A previous study showed that microfiltration was effective to obtain a hibiscus extract with considerable antioxidant content; however, the stability of the final product was not evaluated (Cisse, Vaillant, Soro, Reynes, & Dornier, 2011).

Related to the membrane geometry, hollow fiber membranes present the advantages of greater filtration volumes per membrane module area if compared to flat disks of finite tubes. In addition, laboratory results from flat sheet membranes are not directly scaled up, Mondal and De (2019) affirmed that suitably selected polymeric hollow fiber membranes are efficient for polyphenol purification from green tea extract. Ceramic membranes, also known as mineral or inorganic membranes, are preferred for filtration because of their chemical, mechanical and thermal stability (Cassano, De Luca, Conidi, & Drioli, 2017). Asymmetric ceramic membranes are formed by two main distinct regions: a region with micro-channels of relative high porosity (~ 10 µm) and a spongy-like layer with pores of approximately 0.2 µm. The micro-channels, which are formed as organized structures, are desirable to reduce transmembrane resistance for permeation (Bessa et al., 2019; Gil, Reis, Chadwick, Wu, & Li, 2015). A recent study showed that filtration using an asymmetric hollow ceramic membrane was effective in clarifying genipap fruit extract (Terra, Madrona, Ferreira, Cardoso, & Reis, 2019).

The cost of ceramic membranes is still a drawback for their widespread use in filtration processes. Some studies are reported on the use of low cost mineral materials to produce ceramic membranes at relative low sintering temperatures (Arzani, Mahdavi, Sheikhi, Mohammadi, & Bakhtiari, 2018; Bessa et al., 2019; Bessa, Terra, Cardoso, & Reis, 2017; Ferreira, Bessa, Cardoso, & Reis, 2019; Jamalludin et al., 2018; Kumar, Ghoshal, &

Pugazhenthi, 2015; Xavier et al., 2019). However, the mechanical resistance of these mineral membranes is still a concern. Bessa et al. (2019) reported that the addition of 25 wt% of dolomite (a low-cost ceramic material) to alumina increased the mechanical resistance of pure alumina membranes in 49% due to spinel formation after sintering. The spinel membranes were successfully applied for the treatment of an oily emulsion, with oil rejection of 94.5% (Bessa et al., 2019).

Membrane fouling is also a concern for industrial applications of membrane filtration processes, since drastic flux declines cause process interruptions for membrane cleaning or replacement. The better understand of fouling mechanisms during membrane filtrations is essential to propose optimized process conditions. The literature presents some mathematical models to describe flux declines during membrane filtrations (Iritani, 2013; Jepsen, Bram, Pedersen, & Yang, 2018; Kirschner, Cheng, Paul, Field, & Freeman, 2019; Krippl, Dürauer, & Duerkop, 2020). The mathematical model proposed by Field et al. (1995) is usually applied to indicate the predominant fouling occurrence (cake formation, complete pore blockage, intermediate pore blockage or internal pore blockage) in cross-flow membrane filtrations (Chew, Kilduff, & Belfort, 2020). The flux decline during membrane filtrations of different beverages is frequently described by the model proposed by Field et al. (1995) (Balyan & Sarkar, 2018; Córdova, Astudillo-Castro, Ruby-Figueroa, Valencia, & Soto, 2020; Jain et al., 2018; Magalhães, Sá, Cardoso, & Reis, 2019). Jain et al. (2018) applied the model proposed by Field et al. (1995) to identify fouling occurrences during microfiltration of bitter gourd (*Momordica charantia*) extract through asymmetric polymeric hollow fiber membranes. However, a few earlier attempts were focused on the analysis of fouling occurrences during tea filtration through asymmetric ceramic hollow fiber membranes (Bindes et al., 2020). Also, the model proposed by Field et al. (1995) is able to calculate the flux decline based on a single fouling mechanism, but more than one fouling mechanism may occur during filtration. Mondal and De (2009) and Mondal and De (2010) proposed theoretical models to represent the sequential occurrence of fouling mechanisms for steady state continuous filtrations, which enable to represent membrane fouling mechanisms based on non-dimensional parameters.

In this context, the present work aimed to evaluate the application of filtrations through asymmetric spinel hollow fiber membranes to clarify hibiscus extract with and without pretreatment (centrifugation). The use of asymmetric spinel hollow membranes for tea filtration is innovative and may represents a suitable alternative for the food industry due to the membrane stability and relative high permeate flux. Additionally, here we proposed the application of a low cost ceramic material with outstanding characteristics for producing ceramic hollow fiber membranes. The physico-chemical characteristics of feed and permeate samples were fully evaluated, including extract stability for 20 days of storage under refrigeration. The experimental flux decay was mathematically modeled to investigate fouling occurrences during membrane filtration based on the mathematical models proposed by Field et al. (1995) and Mondal and De (2009).

2. Material and Methods

2.1 Chemicals and reagents

The reagents 6-hydroxy-2,5,7,8-tetramethylchromane-2-carboxylic acid (Trolox), 2,2-diphenyl-1-picrylhydrazyl (DPPH), Folin-Ciocalteu reagent, calcium gallate, 2,4,6-tripyridyl -s-triazine (TPTZ) were obtained from Sigma-Aldrich Chemical Co. (St. Louis, MO, USA). Methanol (chromatography grade) was purchased from Vetec Ltda. (Sao Paulo, Brazil). All other used reagents were of analytical grade.

2.2 Hibiscus Calyx Extract

One lot of dried hibiscus calyx was acquired in the local market (Maringa, Parana – Brazil). The hibiscus calyx was ground in an electric mill (Marconi-MA090/ CFT) and classified according to particle size using the Tyler sieves series and the sieved powder of particle sizes in the range of 0.420 to 0.595 mm was used to continue the experiments.

Hibiscus extract was obtained by ultrasound assisted extraction. Samples were placed in an ultrasonic bath (Ultracleaner 1650 Unique, 40 KHz frequency) at 60 °C for 45 min and the calyx: solvent ratio was 1:10 by using distilled water as solvent (Paraíso et al., 2019). The extract was filtered on a Whatman filter paper to remove rough particles.

2.3 Membrane filtration system

The ceramic membrane was produced by the phase inversion process and using a mixture of 25 wt% of dolomite and 75 wt% of alumina as ceramic powder. After extrusion, the ceramic hollow fiber precursor was sintered at 1250°C and, at this temperature, the mixture of dolomite and alumina reacted to form spinel. Details about membrane production and characteristics are presented by Bessa et al. (2019). Briefly, according to scanning electron microscopy (SEM) images, the sintered hollow fibers presented inner and outer diameters of 0.1566±0.0034 and 0.2020±0.0024 cm, respectively (Bessa et al., 2019). Also, the spinel hollow fibers presented an asymmetric pore distribution with pore sizes ranging from 0.16 to 5.29 µm and a membrane hydraulic permeability of 1188 kg h^{-1} m^2 bar^{-1} (Bessa et al., 2019).

For filtration experiments, four pieces of the spinel hollow fibers were assembled in a plastic tube corresponding to a filtration area of 1.85 x 10^{-4} m^2. The membrane module with the spinel hollow fiber membranes was attached to the cross-flow filtration unit (Milipore Labscale ™ TFF System). The extract was fed from the shell side of the membrane and the permeate was collected from the lumen side. The retentate and permeate streams were returned to the feed tank (total recycle mode). Permeate fluxes were continuously measured until flux stabilization. Filtrations were performed at continuous cross-flow operation mode, room temperature (approximately 25 °C) and at 1 bar of transmembrane pressure. Figure 1 presents a scheme of the membrane filtration unit.

Hibiscus extracts were filtered with and without centrifugation as pretreatment. Centrifugation (Beckman, model Coulter Avanti J25) was carried at 8000 rpm and room temperature (aproximatly 25°C) for 20 min, as suggested by Bindes et al. (2019). Filtration assays were performed in duplicate and the samples were named as: E - Crude Extract, EC - Centrifuged extract, P - Permeate of the crude extract and PC - Permeate of the centrifuged extract.

2.4 Physicochemical analyses of extract and permeate samples

Hibiscus feed extract and permeate samples were analyzed for pH, total soluble solids (TSS), total solids (TS), total phenolic compounds (TPC), total anthocyanins (TA), antioxidant (DPPH and FRAP) and instrumental color.

Values of pH were measured using a PG2000 Digital model pHmeter. Soluble solids contents were measured using a refractometer (HI 96801 Hanna) and were expressed as °Brix. Total solids were analyzed by weighing 5 mL of the sample before and after drying at 105 °C for 24 h (AOAC, 2016).

Determination of total phenolic compounds (TPC) was performed by using the Folin-Ciocalteu assay. Absorbance analysis was performed in a spectrophotometer (UVmini - 1240

Shimadzu) at 725 nm. The content of phenolic compounds was calculated from the standard gallic acid curve ($R^2 = 0.99$) and results were expressed as mg of gallic acid equivalent (GAE) g^{-1} extract (Pierpoint, 2004; Singleton & Rossi, 1965). Determination of total anthocyanin content (TA) was done in a spectrophotometer (UVmini - 1240 Shimadzu) and the absorbance was measured at 535 nm (Lees & Francis, 1972). Total anthocyanin content was expressed as mg cyanidin-3-glucoside (C3G) equivalent 100 g^{-1} extract.

For the determination of antioxidant activity two different methods were used. The reduction of the stable radical DPPH (2,2-diphenyl-1-picrylhydrazyl) was determined according to the methodology described by Thaipong, Boonprakob, Crosby, Cisneros-Zevallos, and Hawkins Byrne (2006). Absorbance was measured at 515 nm and antioxidant activity was calculated from the Trolox standard curve ($R^2 = 0.99$) and expressed in mM Trolox (TE) g^{-1} extract. The Ferric ion reducing antioxidant power (FRAP) was determined according to the methodology described by Pulido, Bravo, and Saura-calixto (2000). The absorbance was measured at 595 nm and the antioxidant activity was calculated from the standard ferrous sulphate curve ($R^2 = 0.99$) and expressed in uM ferrous sulfate (FS) g^{-1} extract.

Color was evaluated using a Minolta® CR400 portable colorimeter using CIEL * a * b * system**,** where: L, represents luminosity on a scale from 0 (black) to 100 (white); a * represents shade ranging from red (0 + a) to green (0 - a) and b * represents shade ranging from yellow (0 + b) to blue (0 - b).

Ultra performance liquid chromatography - mass spectrometer (UPLC-MS/ MS) was used to identify bioactive compounds from hibiscus extract and permeate samples. The extracts were injected in a Bridged Ethane Hybrid (BEH) UPLC Acquity UPLC® system coupled to the Xevo TQD™ triple quadrupole (Milford, MA, USA) mass spectrometer, equipped with a Waters Zspray™ electrospray ionization (ESI) source (Milford, MA, USA). The mobile phase was of a 0.1% formic acid acidified water solution (A) and pure methanol (B) generating a mobile phase at pH 3. The mass spectrometer was operated in positive and negative mode by using the following conditions: 3 kV capillary voltage, cone voltage depends on each molecule, 500 °C desolvation temperature gas, and 800 L h^{-1} flux of desolvation gas, 3,5 mbar collision gas pressure. The analysed molecules were separated on an Acquity UPLC® bridged ethics hybrid (BEH) C18 column (50 mm x 2.1 mm, 1.7 µm). The developed gradient for separation was 0.22 mL min^{-1}, with the following mobile phase mixtures (at volumetric basis): 87A:13B for 0 to 3 min, 35A:65B for 3 to 7.2 min, 0A:100B for 7.2 to 8.3 min. Thereafter, the mobile phase returns to initial conditions generating a total chromatographic run of 12 min. The column was maintained at 40 °C and the injection volume was 4 µL.

The effect of membrane filtration on product stability was also evaluated. Extract and permeate samples were stored at 5°C for 20 days and their content of total phenolic compounds, total anthocyanins and tea cream formation were evaluated. Tea cream solids were determined after 16 h under refrigeration (about 5°C) by centrifuging the sample for 20 min at 5600 rpm to remove insoluble solids. Then, the amount of soluble solids in the supernatant was verified. The difference between the amount of solids in the sample and the supernatant indicates tea cream formation under cooling (Chandini et al., 2013).

2.5 Mathematical Modeling of Flux Decay

The mathematical model proposed in the literature (Field et al., 1995) (Eq. 1) was used to describe fouling mechanisms during cross-flow filtrations of hibiscus extract at total recycle mode.

$$-\frac{dJ}{dt}J^{n-2} = K(J - J_{SS}) \quad (1)$$

where J is the permeate flux (kg h^{-1} m^2), J_{SS} is the flux obtained at steady state (kg h^{-1} m^2), t is the filtration time (h) and K is the adjusted parameter. The values of "n" were fixed according to the fouling mechanism that occurs during membrane filtration (for cake formation n = 0, for complete pore blockage n = 2, for intermediate pore blockage n = 1 and for internal pore blockage n = 1.5).

Equation 1 was numerically solved for each value of "n" by using the Levenberg-Marquardt method in a Fortran program using an integration step of 10^{-3} with an accuracy of 10^{-8}. Values of coefficients of determination (R^2) were used as criteria for data fitting adequacy.

The mathematical model proposed by Mondal and De (2009) was also used to describe fouling mechanisms during cross-flow filtrations of hibiscus extract at total recycle mode. Briefly, the model proposed by Mondal and De (2009) considers that complete pore blocking and cake formation are responsible for fouling mechanisms. The complete pore blocking is the main fouling mechanism from the beginning of filtration up to a time of operation t_1 and the equation proposed by Hermia (1982) with the n exponent equals to 2 (n=0 for complete pore blocking) is used to describe the flux decay. After the membrane pores are blocked by the solution particles, it is assumed that a continuous cake layer is formed on the membrane surface. Thus, for $t>t_1$, the flux decay is modeled by the equation proposed by Field et al. (1995) with the n exponent equals to zero (n=0 for cake formation). This set of equations was solved in order to calculate the transition time from constant pore blocking to the onset of cake formation (t_1) in addition to the complete pore blocking and cake constants (K_1 and K_c, respectively). The set of equations was implemented in R language and a genetic algorithm (Scrucca, 2013) was used to find the optimal parameters with population size, generation, crossover probability and mutation probability fixed at 100, 500, 0.8 and 0.1, respectively, as suggested by Oliveira, Filho, Moruzzi, and De Oliveira (2018).

After calculation of the equations parameters, the non-dimensional parameter G_1, defined as $k_c J_0^2/k_1$, was determined to consider the region of feasible solution in the phase space plot presented by Mondal and De (2009).

The resistance in series model was also used to describe fouling during filtration. The membrane hydraulic resistance (R_M) was determined by filtering distilled water through a new membrane and was calculated according to Eq. 2.

$$R_M = \frac{\Delta P}{J_{w0}\eta_w} \tag{2}$$

where R_M is the membrane hydraulic resistance (m^{-1}), J_{w0} is the water flux through a new membrane ($m\ s^{-1}$), ΔP is the transmembrane pressure (Pa) and η_w is the dynamic viscosity of water (Pa s).

The fouling layer resistance (R_F) was calculated according to Eq. 3 (Ennouri et al., 2015).

$$R_F = \frac{\Delta P}{J_w\eta_w} - R_M \tag{3}$$

where J_w is the water flux through the membrane used for extract filtration ($m\ s^{-1}$).

The fouling index (FI) was estimated by measuring water permeability before and after filtration of hibiscus extract, and fouling index was calculated according to Eq. 4.

$$FI = \left(1 - \frac{L_{w1}}{L_{w0}}\right) 100 \qquad (4)$$

where Lw_0 and Lw_1 are the water permeabilities before and after filtration of hibiscus extract, respectively.

2.6 Membrane characterization

Attenuated Total Reflectance (ATR) was used to investigate membrane functional groups and molecular structures in the membrane surface before and after filtration of hibiscus extract. For this analysis, a Fourier transform infrared spectrometer (Vertex model 70v, Bruker, Germany) coupled to an attenuated total reflectance accessory (Platinum model, Bruker, Germany) was used. The sample was placed over the diamond crystal and each spectrum was measured at an average of 128 scans with a spectral resolution of 4 cm^{-1}. The spectral range of measurement was 4000 to 400 cm^{-1}.

The membrane surface morphology (cross section and outer surface) was evaluated by scanning electron microscopy (SEM) using a JEOL scanning electron microscope (model JSM-6060 LV). The samples were fixed on a metallic support with the aid of a double-sided carbon tape and covered with a thin layer of gold. Visualization was performed in increments of 100 to 5000 times with an excitation voltage of 10 kV.

2.7 Statistical analysis

Analyzes were performed in triplicate and were statistically evaluated by analysis of variance (ANOVA), compared by the Tukey test with a significance level of 5% ($p \leq 0.05$) using the Sisvar 5.6 statistical program.

3. Results and Discussion

3.1 Physicochemical analyzes of extracts and permeates

Table 1 presents the physicochemical characteristics of feed and permeate hibiscus extracts in terms of pH, total soluble solids (TSS), total solids (TS), total phenolic compounds (TPC), total anthocyanins (TA), antioxidant capacities (DPPH and FRAP) and instrumental color. There was no difference between samples regarding to pH values. Terra et al. (2019) also reported no changes in pH and acidity values of genipap extract after filtrations through hollow ceramic fiber membranes.

After centrifugation, TSS and TS values were reduced by 2.4 and 5.3%, respectively (Table 1). Similarly, Bindes et al. (2019) observed that centrifugation decreased TS content in green tea extract by 8.56%. The membrane filtration of crude extract (single process) decreased TSS and TS values by 22.24 and 15.32%, respectively (Table 1). Madrona et al. (2018) showed that the clarification of genipap extract through a 0.8 µm cellulose ester microfiltration membrane reduced TS and TSS contents of feed extract in 19.70 and 33.80%, respectively. The sequential process of centrifugation and membrane filtration was more effective than the single processes in clarifying the hibiscus extract, with a reduction of TS and TSS of 19.82 and 27.12%, respectively (Table 1). A recent study on sequential centrifugation and microfiltration through a 0.22 µm pore size acetate cellulose membrane observed a reduction of 12.93% in TS content in green tea extract (Bindes et al., 2019).

Membrane filtration increased the L value of hibiscus extract. The values of a * and b* also increased after the membrane filtration process, which is a promising result, since the color of food and drinks impacts subsequent perception of taste, flavor, and overall sensory perception (Gous, Almli, Coetzee, & de Kock, 2019). Ennouri et al. (2015) also reported that a ceramic membrane (0.22 µm) was efficient for the clarification of purple carrot juice, obtaining L values of 46 and 65 for extract and permeate samples, respectively.

Centrifugation process did not alter the concentration of bioactive compounds in the extract (equivalent values of TPC, TA, DPPH and FRAP). Membrane filtration without pretreatment retained only 9 and 23% of phenolic and anthocyanin compounds, respectively. Retention of bioactive compounds is not desirable in a clarification process in order to maintain the functional properties of the extract (Bindes et al., 2019). Retention of these compounds occurs partially due to the interaction with other specific compounds (Meija, Parpinello, Versari, Conidi, & Cassano, 2019). Cassano et al., 2019 presented results on the clarification of aqueous extracts from red wine corks through microfiltration using a PVDF hollow fiber membrane and observed a retention of 11.12% of anthocyanins. Meija et al. (2019) also reported similar retention of polyphenol compounds (23%) from red wine cork extract by a 0.15µm PVDF microfiltration membrane.

In order to evaluate the effects of membrane filtration in the antioxidant activity of hibiscus extract, two different methods (DPPH and FRAP) were used due to the fact that antioxidant compounds can act by different radical mechanisms, resulting in different degrees of antioxidant capacity in different trials (Fernández-Moriano, González-Burgos, Divakar, Crespo, & Gómez-Serranillos, 2016). The membrane filtration process caused some reductions in DPPH and FRAP values, but the extract still maintained its antioxidant property after filtrations. Conidi, Cassano, Caiazzo, and Drioli (2017) also reported reductions in antioxidant activity in pomegranate juice after filtration through commercial ultrafiltration membranes.

Bioactive compounds in hibiscus calyx extract and permeate samples were also evaluated by UPLC-MS/ MS (Table 2). The identified compounds were: Cyanidin (m/z

287.1), delphinidin (m/z 303.1), 4-caffeoylquinic acid (m/z 353.0), quercetin hexoside (m/z 463.0), quercetin (m/z 595.0), myricetin (m/z 611.0) and kaempferol (m/z 285.0). These compounds have been identified in previous studies on aqueous and ethanolic extract of hibiscus (Paraíso et al., 2019; Pimentel-Moral et al., 2018; Sinela et al., 2017).

Kaempferol was not identified in the permeate sample of the single filtration process (without centrifugation). Phenolic compounds are amphipathic molecules with hydrophobic and hydrophilic (acidic) phenolic hydroxyl groups. Membrane adsorption and complexation with other compounds involve hydrophobic interactions and hydrogen bond formation (Cassano et al., 2017). This result suggests that kaempferol may have interacted with the membrane or other compounds to form large particles and, thus, was unable to permeate the pores of the ceramic membrane. Pretreatment with centrifugation decreased solid content (Table 1) and probably reduced the possibility of kaempferol interaction with other compounds. Therefore, although the bioactive compounds are much smaller than the average pore size of the used ceramic membrane, the interactions of these compounds between each other and with the membrane surface and pores may play a key role in membrane fouling and loss of such compounds (Vernhet & Moutounet, 2002).

3.2 Flux analyses for hibiscus extract filtrations

Figure 2 shows the permeate flux as a function of time for extract filtration with and without centrifugation through the asymmetric ceramic hollow membrane at 1 bar of transmembrane pressure. There was a significant improvement in permeate flux with pretreatment (centrifugation). For the extract without centrifugation, the initial flux was 460.23 kg m^{-2} h^{-1} and with centrifugation the initial flux was 694.79 kg m^{-2} h^{-1}, representing a flux increase of 51%. The stabilized permeate flux for the extract without centrifugation was 109.15 kg $m^{-2} h^{-1}$ and, with centrifugation, the stabilized flux was 142.58 kg $m^{-2} h^{-1}$, representing a flux increase of 31%. Domingues, Ramos, Luiz, and Reis (2014) also showed that the pretreatment by centrifugation resulted in permeate fluxes of passion fruit juice through a polyetherimide hollow fiber membrane of 0.40 µm higher than without centrifugation. Pretreatments such as centrifugation play an important role in removing suspended solids, preventing rapid flux decrease during membrane filtration (Bindes et al., 2019).

The characteristics of the spinel membrane probably enabled the achievement of a relatively high permeate flux. The organized pore micro-channels with approximately 5 µm (Bessa et al., 2019) promoted the permeation through the membrane while the sponge-like layer was responsible for membrane selectivity. Extract characteristics also influenced permeate flux so that a comparison with other results reported in the literature is not direct. Domingues et al. (2014) reported a permeate flux of 19.5 kg $m^{-2} h^{-1}$ for the permeation of passion fruit juice through a membrane of 0.3 µm. Madrona et al. (2018) reported a permeate flux of genipap fruit extract through a flat polymeric membrane of 0.22 µm of 9.50 kg $m^{-2} h^{-1}$. Terra et al. (2019) used an alumina hollow fiber membrane for genipap fruit extract filtrations, which resulted in a stabilized flux of 191 kg $m^{-2} h^{-1}$, which is quite similar to the value found in this work.

The experimental flux data were adjusted to the mathematical model proposed by Field et al. (1995) to describe fouling mechanisms. A sharp decrease in permeate flux (with or without centrifugation) was observed in the first 20 min of filtration, followed by a period of stabilization. Similar results were observed during filtration of green tea in microfiltration membranes (Sousa et al., 2016) and yerba mate extract (Gerke, Hamerski, Scheer, & Silva, 2017).

Figure 2 shows that the mechanism that most contributed to flux decline was complete pore blockage (n = 2) for both filtrations (with and without centrifugation). Results presented in Table 3 show that the best fitting was achieved for n=2 (complete pore blockage). However, all the other fouling mechanisms also described satisfactorily the experimental flux data, with R^2 values greater than 0.97. The worst adjustment (R^2=0.9733) was observed for cake formation when filtering the centrifuged extract. The relative large pore size of the used membrane (0.16 to 5.29 µm) contributed to fouling occurrences due to pore blockage. Also, extract centrifugation mitigated cake formation due to the removal of large particles. Madrona et al. (2018) evaluated the microfiltration of genipap extract through cellulose ester membranes (0.8, 0.3 and 0.22 µm) at 1 bar of transmembrane pressure and reported that the major fouling mechanism was cake formation. Balyan, Verma, and Sarkar (2019) evaluated the purification of jamun leaf extract by using microfiltration membranes (0.1, 0.22, 0.45 and 0.8 µm) and noted that decrease in permeate flux was attributed to the blocking of pores followed by gradual cake formation. These results suggest that fouling mechanisms during membrane filtration generally depend on specific interactions between membrane and different solutes in the feed stream, membrane material and pore size, operating parameters and the nature of the solutes to be filtered (Balyan et al., 2019; Cassano et al., 2017).

The model proposed by Mondal and De (2009) was also applied to represent the flux decay during the cross-flow membrane filtration of hibiscus extract through the produced spinel hollow fiber membrane at total recycle mode. Figure 3 presents experimental and calculated (S. Mondal & De, 2009) flux decays for membrane filtrations of centrifuged and non-centrifuged hibiscus extracts. The model proposed by Mondal and De (2009) described satisfactorily experimental flux decays with R^2 values of 0.9901 and 0.9836 for extract filtrations with and without centrifugation, respectively. According to the model proposed by

Mondal and De (2009), membrane fouling is composed by sequential mechanisms of total pore blocking and cake formation. The model is able to predict the transition time between total pore blocking and cake formation. Table 4 presents the calculated transition time from complete pore blocking to the onset of cake formation (t_1) and the constants of complete pore blocking and cake formations (k_1 and k_c, respectively).

After calculation of the equations parameters, the non-dimensional parameter G_1, defined as $k_cJ_0^2/k_1$, was determined to consider the region of feasible solution in the phase space plot presented by Mondal and De (2009).

The calculated intrinsic membrane resistance (R_M) was $2.7x10^{11}$ m^{-1}. Ennouri et al. (2015) reported a R_M value of $4.43x10^{12}$ m^{-1} for a ceramic membrane with an average pore size of 0.22 µm. Intrinsic membrane resistance is directly related to membrane permeability, and lower resistance is favorable for higher permeation. After the membrane was used to filter hibiscus extract, the fouling layer resistance was $3.42x10^{12}$ and $0.93x10^{12}$ m^{-1} for extracts without and with centrifugation, respectively. In addition, the fouling index (FI) values for the extract without and with centrifugation were 87.71 and 70.69 %, respectively. Meija et al (2019) showed that the fouling index was about 50% in the clarification of red wine cork extract through a PVDF microfiltration hollow fiber membrane. This result suggests that centrifugation decreased resistance and fouling index, mainly because centrifugation reduced the solid content of hibiscus extract, as shown in Table 1.

3.3 Membrane characterizations

The membranes before and after extract filtration were characterized by FTIR-ATR spectroscopy (Figure 4) to determine the possible compounds present in the membrane, which were responsible for fouling. The broad band in the region 3421 cm-

^{1} corresponds to the stretching vibration of the O–H bond in hydroxyl groups, which had the highest intensity in the used membrane because of the adherence of polyphenolic compounds present in hibiscus extract on the membrane surface (Cassano et al., 2017; Li et al., 2018). The band at 1635 cm^{-1} corresponds to the C–N–H stretch that was assigned to the amino group, and therefore corresponds to the presence of proteins and/ or amino acids (Shi et al., 2019). The peak at 1232 cm^{-1} corresponds to the C–O elongation that was attributed to polysaccharides. The bands at 1786 cm^{-1} and 1193 cm^{-1} are assigned to the C=O and C– O–C stretch vibrations, respectively (Haddad, Mohammed, & Aliy, 2011; Lee, Vengadaesvaram, Arof, & Abidin, 2013; Pappas, Tarantilis, & Polissiou, 1998). The bands at 700-400 cm^{-1} were attributed to the membrane material (Li et al., 2018). These results indicate that polysaccharides, proteins and phenolic compounds are responsible for membrane fouling. Jain et al. (2018) also related the presence of polyphenols by FTIR analysis on the membrane surface after microfiltration of mitter gourd extract.

The asymmetric structure of the ceramic hollow fibers before hibiscus extract filtration is presented in Figure 5 c. The cross-sectional area of the hollow fiber presented micro-channels (fingers) through all the extension. This is due to the phase inversion technique for membrane synthesis, wherein the micro-channels can be distinguished at various levels, in terms of length, diameter and density of the spinel hollow fiber asymmetric membrane (Bessa et al., 2019; Lee, Wang, Wu, & Li, 2015).

After filtering hibiscus extract through the membrane (Figure 5 b), the membrane outer surface becomes completely closed, confirming that a cake layer was deposited on the membrane outer surface. This structure contains mainly polysaccharides, proteins, and phenolic compounds that probably caused membrane fouling, as confirmed by FTIR results (Figure 4). Furthermore, the cross-sectional view of the used membrane (Figure 5

d) presented a cake layer of 10.2±1.8 μm (measured with the software ImageJ in the SEM image). This cake layer was formed due to particle deposition in the membrane surface, while pore blockage was probably caused by smaller particles that were trapped in the membrane pores (Shi et al., 2019). Similar behavior was observed in a previous study with the filtration of sugarcane juice through ultrafiltration ceramic membranes (Li et al., 2018) and with microfiltration of mitter gourd extract through polymeric hollow fiber membranes (Jain et al., 2018).

3.4 Stability tests

Figure 6 shows the stability of the clarified hibiscus extract obtained in terms of concentrations of total anthocyanin (TA) and total phenolic compounds (TPC) and tea cream formation for 20 days of storage. The concentration of anthocyanins (Figure 6 a) decreased 23% in the crude extract and 18 % in the permeate for 20 days of storage. Sinela et al. (2017) also reported decreases in anthocyanins during storage of hibiscus extract for 60 days at 4°C. Anthocyanin degradation leads to the cleavage of cyanidin and delphinidin, thus forming the products protocatechuic acid and gallic acid, respectively.

Regarding to phenolic compounds (Figure 6 b), a decrease of 34% and 14% was observed for crude extract and permeate samples, respectively. In addition, there was a sharp decrease in total polyphenol content for the first 10 days of storage for the permeate sample and, then, the values remained constant until 20 days of storage. Similar behavior of phenolic compound degradations was observed in green tea extract storage, where losses of these compounds were greater for crude extract than for permeate (Sousa et al., 2016). The decrease in total phenolic concentration is probably due to polyphenol-protein interactions, which may cause tea cream formation (Todisco, Tallarico, & Gupta, 2002).

The sequential process of centrifugation and membrane filtration reduced tea cream formation (Figure 6 c) in hibiscus extract by 43.1% after 20 days. Bindes et al. (2019) evaluated the stability of green tea extract and observed the reduction of tea cream formation by 82% after microfiltration through a 0.22 μm membranes. Chandini et al. (2013) also showed a significant improvement in decreasing tea cream formation during 30 days of storage after green tea filtration through 0.20 and 0.45 μm membranes. In this sense, these results suggest that membrane filtration can retain compounds responsible for interaction with phenolic compounds and consequently formation of tea cream. Reduction in the concentration of anthocyanins and polyphenols was equivalent in the single membrane filtration process and in the sequential process of centrifugation and membrane filtration. The sequential process was more effective in reducing tea cream formation than the single membrane filtration.

4. Conclusion

Application of centrifugation as a pretreatment for membrane filtration resulted in higher permeate fluxes of hibiscus extract and in a clarified product. Polysaccharides, proteins and phenolic compounds were probably responsible for fouling, as confirmed by FTIR analysis on the membrane surface used for extract filtration.

Sequential process (centrifugation and membrane filtration) was able to significantly reduce values of total soluble solids and total solids and to increase extract luminosity. In addition, the retention of phenolic and anthocyanin compounds was lower than 23%, so that the proposed clarification process did not compromise the functional characteristics of hibiscus extract. The following individual bioactive compounds were identified after the sequential process: cyanidin (m/z 287.1), delphinidin (m/z 303.1), 4-caffeoylquinic acid (m/z

353.0), quercetin hexoside (m/z 463.0), quercetin (m/z 595.0), myricetin (m/z 611.0) and kaempferol (m/z 285.0).

Finally, it is important to highlight that the centrifuged and filtered extract showed greater stability than the crude extract after 20 days of storage at 5°C, reducing tea cream formation in 43.1%. Thus, the sequential process of centrifugation and filtration through asymmetric spinel hollow fiber membranes can be applied to produce a ready-to-drink hibiscus tea with high antioxidant content.

5. Acknowledgements

We acknowledge financial support from CAPES (Coordenação de Aperfeiçoamento de Pessoal de Nível Superior), Fapemig, and CNPq (Conselho Nacional de Desenvolvimento Científico e Tecnológico).

6. Author's contributions

Carolina Moser Paraíso: Conceptualization; Data curation; Formal analysis; Investigation; Methodology; Software; Writing-original draft; Writing-review & editing. Suelen Siqueira dos Santos: Formal analysis; Investigation; Methodology. Lidiane Pereira Bessa: Formal analysis; Investigation; Methodology. Ana Paula Lopes: Formal analysis; Investigation; Methodology. Camilla Yara Langer Ogawa: Formal analysis; Investigation; Methodology. Silvio Cláudio da Costa: Formal analysis; Investigation; Methodology. Miria Hespanhol Miranda Reis: Conceptualization; Data curation; Formal analysis; Funding acquisition; Investigation; Methodology; Software; Writing-original draft; Writing-review & editing. Ubirajara Coutinho Filho: Data curation; Investigation; Methodology; Software. Francielle Sato: Formal analysis; Investigation; Methodology. Jesuí V. Visentainer: Formal analysis;

Investigation; Methodology. Grasiele Scaramal Madrona: Conceptualization; Data curation; Formal analysis; Funding acquisition; Investigation; Methodology; Project administration; Software; Writing-original draft; Writing-review & editing.

7. Conflict of interest

The authors have declared no conflicts of interest for this article

8. References

AOAC. (2016). Official Methods of Analysis, 20th edition. *Association of Official Analytical Chemists*.

Arzani, M., Mahdavi, H. R., Sheikhi, M., Mohammadi, T., & Bakhtiari, O. (2018). Ceramic monolith as microfiltration membrane: Preparation, characterization and performance evaluation. *Applied Clay Science*, **161**, 456–463. https://doi.org/10.1016/j.clay.2018.05.021

Balyan, U., & Sarkar, B. (2018). Analysis of flux decline using sequential fouling mechanisms during concentration of Syzygium cumini (L.) leaf extract. *Chemical Engineering Research and Design*, **130**, 167–183. https://doi.org/10.1016/j.cherd.2017.12.015

Balyan, U., Verma, S. P., & Sarkar, B. (2019). Phenolic compounds from Syzygium cumini (L.) Skeels leaves: Extraction and membrane purification. *Journal of Applied Research on Medicinal and Aromatic Plants*, **12**, 43–58. https://doi.org/10.1016/j.jarmap.2018.12.002

Bessa, L. P., Ferreira, E. de P., Magalhães, F. de S., Ferreira, F. B., Cardoso, V. L., & Reis, M. H. M. (2019). Micro-structured and reinforced spinel hollow fiber membranes:

Influence of sintering temperature and ceramic powder composition. *Ceramics International*, **45**(17), 23632–23642. https://doi.org/10.1016/j.ceramint.2019.08.075

Bessa, L. P., Terra, N. M., Cardoso, V. L., & Reis, M. H. M. (2017). Macro-porous dolomite hollow fibers sintered at different temperatures toward widened applications. *Ceramics International*, **43**(18), 16283–16291. https://doi.org/10.1016/j.ceramint.2017.08.214

Bindes, M. M. M., Cardoso, V. L., Reis, M. H. M., & Boffito, D. C. (2019). Maximisation of the polyphenols extraction yield from green tea leaves and sequential clarification. *Journal of Food Engineering*, **241**, 97–104. https://doi.org/10.1016/j.jfoodeng.2018.08.006

Bindes, M. M. M., Terra, N. M., Patience, G. S., Boffitoorcid, D. C., Cardoso, V. L., & Reis, M. H. M. (2020). Asymmetric Al2O3 and PES/Al2O3 hollow fiber membranes for green tea extract clarification. *Journal of Food Engineering*, **277**, 109889. https://doi.org/10.1016/j.jfoodeng.2019.109889

Cassano, A., Bentivenga, A., Conidi, C., Galiano, F., Saoncella, O., & Figoli, A. (2019). Membrane-Based Clarification and Fraction of Red Wine Lees Aqueous Extracts. *Polymers*, **11**(7), 1089. https://doi.org/10.3390/polym11071089

Cassano, A., De Luca, G., Conidi, C., & Drioli, E. (2017). Effect of polyphenols-membrane interactions on the performance of membrane-based processes. A review. *Coordination Chemistry Reviews*, **351**, 45–75. https://doi.org/10.1016/j.ccr.2017.06.013

Chandini, S. K., Rao, L. J., & Subramanian, R. (2013). Membrane Clarification of Black Tea Extracts. *Food and Bioprocess Technology*, ***6***(8), 1926–1943. https://doi.org/10.1007/s11947-012-0847-0

Chew, J. W., Kilduff, J., & Belfort, G. (2020). The behavior of suspensions and macromolecular solutions in crossflow microfiltration: An update. *Journal of*

Membrane Science, **601**, 117865. https://doi.org/10.1016/j.memsci.2020.117865

Cid-Ortega, S., & Guerrero-Beltrán, J. A. (2015). Roselle calyces (Hibiscus sabdariffa), an alternative to the food and beverages industries : a review. *Journal of Food Science and Technology*, **52**, 6859–6869. https://doi.org/10.1007/s13197-015-1800-9

Cisse, M., Vaillant, F., Soro, D., Reynes, M., & Dornier, M. (2011). Crossflow microfiltration for the cold stabilization of roselle (Hibiscus sabdariffa L .) extract. *Journal of Food Engineering*, **106**(1), 20–27. https://doi.org/10.1016/j.jfoodeng.2011.04.001

Conidi, C., Cassano, A., Caiazzo, F., & Drioli, E. (2017). Separation and purification of phenolic compounds from pomegranate juice by ultrafiltration and nanofiltration membranes. *Journal of Food Engineering*, **195**, 1–13. https://doi.org/10.1016/j.jfoodeng.2016.09.017

Córdova, A., Astudillo-Castro, C., Ruby-Figueroa, R., Valencia, P., & Soto, C. (2020). Recent advances and perspectives of ultrasound assisted membrane food processing. *Food Research International*, **133**, 109163. https://doi.org/10.1016/j.foodres.2020.109163

Da-costa-rocha, I., Bonnlaender, B., Sievers, H., Pischel, I., & Heinrich, M. (2014). Hibiscus sabdariffa L . – A phytochemical and pharmacological review. *Food Chemistry*, **165**, 424–443. https://doi.org/10.1016/j.foodchem.2014.05.002

Domingues, R. C. C., Ramos, A. A., Luiz, V., & Reis, M. H. M. (2014). Microfiltration of passion fruit juice using hollow fibre membranes and evaluation of fouling mechanisms, **121**, 73–79. https://doi.org/https://doi.org/10.1016/j.jfoodeng.2013.07.037

Ennouri, M., Ben Hassan, I., Ben Hassen, H., Lafforgue, C., Schmitz, P., & Ayadi, A. (2015). Clarification of purple carrot juice: analysis of the fouling mechanisms and evaluation of the juice quality. *Journal of Food Science and Technology*, **52**(5), 2806–2814. https://doi.org/10.1007/s13197-014-1323-9

Fernández-Moriano, C., González-Burgos, E., Divakar, P. K., Crespo, A., & Gómez-Serranillos, M. (2016). Evaluation of the Antioxidant Capacities and Cytotoxic Effects of Ten Parmeliaceae Lichen Species. *Evidence-Based Complementary and Alternative Medicine*, **2016**, 1–11. https://doi.org/htpp://dx.doi.org/10.1155/2016/3169751

Ferreira, E. de P., Bessa, L. P., Cardoso, V. L., & Reis, M. H. M. (2019). Influence of sintering temperature on the morphology of ceramic hollow fibers prepared from niobium pentoxide. *International Journal of Applied Ceramic Technology*, **16**(2), 781–790. https://doi.org/10.1111/ijac.13118

Field, R. W., Wu, D., Howell, J. A., & Gupta, B. B. (1995). Critical flux concept for microfiltration fouling. *Journal of Membrane Science*, **100**(3), 259–272. https://doi.org/10.1016/0376-7388(94)00265-Z

Gerke, I. B. B., Hamerski, F., Scheer, A. P., & Silva, V. R. (2017). Clarification of crude extract of yerba mate (Ilex paraguariensis) by membrane processes: Analysis of fouling and loss of bioactive compounds. *Food and Bioproducts Processing*, **102**, 204–212. https://doi.org/10.1016/j.fbp.2016.12.008

Gil, A. G., Reis, M. H. M., Chadwick, D., Wu, Z., & Li, K. (2015). A highly permeable hollow fibre substrate for Pd/Al2O3 composite membranes in hydrogen permeation. *International Journal of Hydrogen Energy*, **40**(8), 3249–3258. https://doi.org/10.1016/j.ijhydene.2015.01.021

Gous, A. G. S., Almli, V. L., Coetzee, V., & de Kock, H. L. (2019). Effects of Varying the Color, Aroma, Bitter, and Sweet Levels of a Grapefruit-Like Model Beverage on the Sensory Properties and Liking of the Consumer. *Nutrients*, **11**(2), 464.

https://doi.org/10.3390/nu11020464

Haddad, H. H., Mohammed, H. K., & Aliy, N. A. K. A. (2011). Synthesis , Characterzation and analytical study of polymer derive from extracted (Hibiscus Sabdariffa) leaves plant with 8-hydroxyquinoline. *Journal of Kerbala University*, **9**(4), 53–53.

Hermia, J. (1982). Constant Pressure Blocking Filtration Laws - Application To Power-law Non-newtonian Fluids. *Instituion of Chemical Engineers Transactions*, **60**(3), 183–287.

Iritani, E. (2013). A Review on Modeling of Pore-Blocking Behaviors of Membranes During Pressurized Membrane Filtration. *Drying Technology*, **31**(2), 146–162. https://doi.org/10.1080/07373937.2012.683123

Jain, A., Sengupta, S., & De, S. (2018). Fundamental Understanding of Fouling Mechanisms During Microfiltration of Bitter Gourd (Momordica charantia) Extract and Their Dependence on Operating Conditions. *Food and Bioprocess Technology*, **11**(5), 1012–1026. https://doi.org/10.1007/s11947-018-2074-9

Jamalludin, M. R., Harun, Z., Othman, M. H. D., Hubadillah, S. K., Yunos, M. Z., & Ismail, A. F. (2018). Morphology and property study of green ceramic hollow fiber membrane derived from waste sugarcane bagasse ash (WSBA). *Ceramics International*, **44**(15), 18450–18461. https://doi.org/10.1016/j.ceramint.2018.07.063

Jepsen, K., Bram, M., Pedersen, S., & Yang, Z. (2018). Membrane Fouling for Produced Water Treatment: A Review Study From a Process Control Perspective. *Water*, **10**(7), 847. https://doi.org/10.3390/w10070847

Kirschner, A. Y., Cheng, Y. H., Paul, D. R., Field, R. W., & Freeman, B. D. (2019). Fouling mechanisms in constant flux crossflow ultrafiltration. *Journal of Membrane Science*, **574**, 65–75. https://doi.org/10.1016/j.memsci.2018.12.001

Krippl, M., Dürauer, A., & Duerkop, M. (2020). Hybrid modeling of cross-flow filtration:

Predicting the flux evolution and duration of ultrafiltration processes. *Separation and Purification Technology*, **248**, 117064. https://doi.org/10.1016/j.seppur.2020.117064

Kumar, R. V., Ghoshal, A. K., & Pugazhenthi, G. (2015). Elaboration of novel tubular ceramic membrane from inexpensive raw materials by extrusion method and its performance in microfiltration of synthetic oily wastewater treatment. *Journal of Membrane Science*, **490**, 92–102. https://doi.org/10.1016/j.memsci.2015.04.066

Lee, M., Wang, B., Wu, Z., & Li, K. (2015). Formation of micro-channels in ceramic membranes - Spatial structure, simulation, and potential use in water treatment. *Journal of Membrane Science*, **483**, 1–14. https://doi.org/10.1016/j.memsci.2015.02.023

Lee, S. V., Vengadaesvaram, B., Arof, A. K., & Abidin, Z. H. Z. (2013). Characterisation of poly (acrylamide-co-acrylic acid) mixed with anthocyanin pigment from hibiscus sabdariffa l . *Pigment & Resin Technology*, **2**, 9420. https://doi.org/10.1108/03699421311301089

Lees, D. H., & Francis, F. J. (1972). Standardization of pigment analyses in cranberries. *Hortscience*, **7**, 83–84.

Li, W., Ling, G., Lei, F., Li, N., Peng, W., Li, K., … Zhang, Y. (2018). Ceramic membrane fouling and cleaning during ultrafiltration of limed sugarne juice. *Separation and Purification Technology*, **190**(1), 9–24. https://doi.org/10.10.1016/j.seppour.2017.08.046

Madrona, G. S., Terra, N. M., Filho, U. C., Santana, F. De, Cardoso, V. L., & Reis, M. H. M. (2018). Purification of phenolic compounds from genipap (Genipa americana L .) extract by the ultrasound assisted ultrafiltration process. *Acta Scientiarum*, **41**, 1–10. https://doi.org/10.4025/actascitechnol.v41i1.35571

Magalhães, F. de S., Sá, M. de S. M., Cardoso, V. L., & Reis, M. H. M. (2019). Recovery of phenolic compounds from pequi (Caryocar brasiliense Camb.) fruit extract by membrane filtrations: Comparison of direct and sequential processes. *Journal of Food Engineering*, **257**, 26–33. https://doi.org/10.1016/j.jfoodeng.2019.03.025

Meija, J. A. A., Parpinello, G. P., Versari, A., Conidi, C., & Cassano, A. (2019). Microwave-assisted extraction and membrane-based separation of biophenols from red wine lees. *Food and Bioproducts Processing*, **117**, 74–83. https://doi.org/10.1016/j.fbp.2019.06.020

Mondal, M., & De, S. (2019). Purification of Polyphenols from Green Tea Leaves and Performance Prediction Using the Blend Hollow Fiber Ultrafiltration Membrane. *Food and Bioprocess Technology*, **12**(6), 933–953. https://doi.org/10.1007/s11947-019-02262-6

Mondal, S., & De, S. (2009). Generalized criteria for identification of fouling mechanism under steady state membrane filtration. *Journal of Membrane Science*, **344**(1–2), 6–13. https://doi.org/10.1016/j.memsci.2009.08.015

Mondal, S., & De, S. (2010). A fouling model for steady state crossflow membrane filtration considering sequential intermediate pore blocking and cake formation. *Separation and Purification Technology*, **75**(2), 222–228. https://doi.org/10.1016/j.seppur.2010.07.016

Oliveira, A. da S. L., V. D. S., Filho, U. C., Moruzzi, R. B., & De Oliveira, A. L. (2018). Neural network for fractal dimension evolution. *Water Science and Technology*, **78**(4), 795–802. https://doi.org/10.2166/wst.2018.349

Pappas, C., Tarantilis, P. A., & Polissiou, M. (1998). Determination of Kenaf (Hibiscus cannabinus L .) Lignin in Crude Plant Material Using Diffuse Reflectance Infrared Fourier Transform Spectroscopy. *Applied Spectroscopy*, **52**(11), 1399–1402. https://doi.org/https://doi.org/10.1366/0003702981943013

Paraíso, C. M., dos Santos, S. S., Correa, V. G., Magon, T., Peralta, R. M., Visentainer, J. V., & Madrona, G. S. (2019). Ultrasound assisted extraction of hibiscus (Hibiscus sabdariffa L.) bioactive compounds for application as potential functional ingredient. *Journal of Food Science and Technology*, **56**(10), 4667–4677. https://doi.org/10.1007/s13197-019-03919-y

Pierpoint, W. S. (2004). The extraction of enzymes from plant tissues rich in phenolic compounds. *Methods in Molecular Biology*, *244*, 65–74. https://doi.org/10.1385/1-59259-655-x:65

Pimentel-Moral, S., Borrás-Linares, I., Lozano-Sánchez, J., Arráez-Román, D., Martínez-Férez, A., & Segura-Carretero, A. (2018). Microwave-assisted extraction for Hibiscus sabdariffa bioactive compounds. *Journal of Pharmaceutical and Biomedical Analysis*, **156**, 313–322. https://doi.org/10.1016/j.jpba.2018.04.050

Pulido, R., Bravo, L., & Saura-calixto, F. (2000). Antioxidant activity of dietary polyphenols as determined by a modified ferric reducing/ antioxidant power assay. Journal of Agricultural and. *Food Chemistry*, **48**, 3396–3402. https://doi.org/10.1021/jf9913458

Riaz, G., & Chopra, R. (2018). A review on phytochemistry and therapeutic uses of Hibiscus sabdariffa L. *Biomedicine and Pharmacotherapy*, **102**, 575–586. https://doi.org/10.1016/j.biopha.2018.03.023

Scrucca, L. (2013). GA: A package for genetic algorithms in R. *Journal of Statistical Software*, **53**(4), 1–37. https://doi.org/10.18637/jss.v053.i04

Shi, C., Rackemann, D. W., Moghaddam, L., Wei, B., Li, K., Lu, H., … Doherty, W. O. S. (2019). Ceramic membrane filtration of factory sugarcane juice: Effect of pretreatment on permeate flux, juice quality and fouling. *Journal of Food Engineering*, **243**, 101–113. https://doi.org/10.1016/j.jfoodeng.2018.09.012

Sinela, A., Rawat, N., Mertz, C., Achir, N., Fulcrand, H., & Dornier, M. (2017). Anthocyanins degradation during storage of Hibiscus sabdariffa extract and evolution of its degradation products. *Food Chemistry*, **214**, 234–241. https://doi.org/10.1016/j.foodchem.2016.07.071

Singleton, V. L., & Rossi, J. A. (1965). Colorimetry of Total Phenolics with Phosphomolybdic-Phosphotungstic Acid Reagents. *American Journal of Enology and Viticulture*, **16**(3), 144–158.

Sousa, L. dos S., Cabral, B. V., Madrona, G. S., Cardoso, V. L., & Reis, M. H. M. (2016). Purification of polyphenols from green tea leaves by ultrasound assisted ultrafiltration process. *Separation and Purification Technology*, **168**, 188–198. https://doi.org/10.1016/j.seppur.2016.05.029

Terra, N. M., Madrona, G. S., Ferreira, F. B., Cardoso, V. L., & Reis, M. H. M. (2019). High Performance of Asymmetric Alumina Hollow Fiber Membranes for the Clarification of Genipap (Genipa americana L.) Fruit Extract. *Food and Bioprocess Technology*, **12**(1), 27–38. https://doi.org/10.1007/s11947-018-2185-3

Thaipong, K., Boonprakob, U., Crosby, K., Cisneros-Zevallos, L., & Hawkins Byrne, D. (2006). Comparison of ABTS, DPPH, FRAP, and ORAC assays for estimating antioxidant activity from guava fruit extracts. *Journal of Food Composition and Analysis*, **19**, 669–675. https://doi.org/10.1016/j.jfca.2006.01.003

Todisco, S., Tallarico, P., & Gupta, B. B. (2002). Mass transfer and polyphenols retention in the clarification of black tea with ceramic membranes. *Innovative Food Science and Emerging Technologies*, **3**(3), 255–262. https://doi.org/10.1016/S1466-8564(02)00046-2

Vernhet, A., & Moutounet, M. (2002). Fouling of organic microfiltration membranes by wine constituents: importance, relative impact of wine polysccharides and polyphenols and incidence of membrane properties. *Journal of Membrane Science*, **201**(1–2), 103–122. https://doi.org/10.1016/S0376-7388(01)00723-2

Xavier, L. A., de Oliveira, T. V., Klitzke, W., Mariano, A. B., Eiras, D., & Vieira, R. B. (2019). Influence of thermally modified clays and inexpensive pore-generating and strength improving agents on the properties of porous ceramic membrane. *Applied Clay Science*, **168**, 260–268. https://doi.org/10.1016/j.clay.2018.11.025

Table 1 Physicochemical characteristics of hibiscus extract and permeate samples

Parameter	E	P	EC	PC
pH	$2.70^{a} \pm 0.00$	$2.69^{a} \pm 0.01$	$2.70^{a} \pm 0.01$	$2.69^{a} \pm 0.01$
TSS (°Brix)	$5.53^{a} \pm 0.06$	$4.30^{c} \pm 0.00$	$5.40^{b} \pm 0.00$	$4.03^{d} \pm 0.06$
TS (mg/L)	$47120^{a} \pm 141$	$39900^{c} \pm 56$	$44610^{b} \pm 155$	$37780^{d} \pm 197$
TPC (mg EAG/g)	$2.72^{a} \pm 0.03$	$2.49^{b} \pm 0.06$	$2.73^{a} \pm 0.01$	$2.47^{b} \pm 0.03$
TA (mg C3G/100g)	$366.61^{a} \pm 0.70$	$279.53^{a} \pm 0.72$	$366.85^{a} \pm 0.36$	$281.06^{a} \pm 0.72$
DPPH (mM TE/ g)	$103.95^{a} \pm 1.02$	$90.07^{b} \pm 0.71$	$105.17^{a} \pm 1.18$	$90.69^{b} \pm 1.09$
FRAP (μM SF/ g)	$224.22^{a} \pm 1.13$	$194.78^{b} \pm 0.68$	$226.94^{a} \pm 0.91$	$198.94^{b} \pm 1.58$
L	$15.69^{c} \pm 0.00$	$20.72^{b} \pm 0.01$	$15.74^{c} \pm 0.57$	$22.03^{a} \pm 0.01$
a*	$3.12^{c} \pm 0.03$	$10.12^{b} \pm 0.01$	$3.17^{c} \pm 0.03$	$14.69^{a} \pm 0.03$
b*	$4.08^{c} \pm 0.03$	$6.55^{b} \pm 0.01$	$4.30^{c} \pm 0.03$	$10.87^{a} \pm 0.01$

Mean values denoted by a different letter along a line are significantly different at $p \leq 0.05$.

Total soluble solids (TSS), total solids (TS), total phenolic compounds (TPC), total anthocyanin (TA).

Table 2 Identification of bioactive compounds in extracts and permeates

Identification attempt	TR (min)	m/z	Fragments	Cone (v)	Energy Collision (v)	Mode	Samples			
							E	P	EC	PC
Cyanidin	2.65	287.1	121.0 137.1 213.0	70 70 70	45 45 45	ES +	+	+	+	+
Delphinidin	1.53	303.1	152.9 229.0 257.0	80 80 80	50 45 40	ES +	+	+	+	+
4-Caffeoylquinic acid	0.97	353.0	173.0	30	20	ES -	+	+	+	+
Quercetin Hexoside	4.01	463.0	301.0	30	20	ES -	+	+	+	+
Quercetin	1.61	595.0	300.0 463.0	30 30	20 20	ES -	+	+	+	+
Myricetin	3.24	611.0	316.0	30	25	ES -	+	+	+	+
Kaempferol	5.18	285.0	92.9 255.9	58	35	ES-	+	-	+	+

Table 3 Values of coefficient of determination (R^2) for the adjustment of experimental flux data for each fouling mechanism according to the model proposed by Field et al. (1995).

Fouling mechanism	With centrifugation	Without centrifugation
Cake formation (n=0)	0.9733	0.9860
Partial pore blocking (n=1)	0.9908	0.9963
Internal pore blocking (n=1.5)	0.9960	0.9987
Complete pore blocking (n=2)	0.9986	0.9989

Table 4 Calculated parameters (transition time from complete pore blocking to the onset of cake formation (t_1) and constants of complete pore blocking and cake formations (k_1 and k_c, respectively)) according to the model proposed by Mondal and De (2009) for describing fouling mechanisms during filtrations of hibiscus extract with and without centrifugation.

Extract	t_1 (min)	k_1 (min^{-1})	k_c (min m^{-2})	J_{ss}/J_0	$G_1=k_cJ_0^2/k_1$
Centrifuged	25.3	3.78x10-2	1.59x105	0.20	565
Non-centrifuged	27.6	2.58x10-2	2.72x105	0.23	632

J_{ss} is the steady state permeate flux and J_0 is the initial permeate flux.

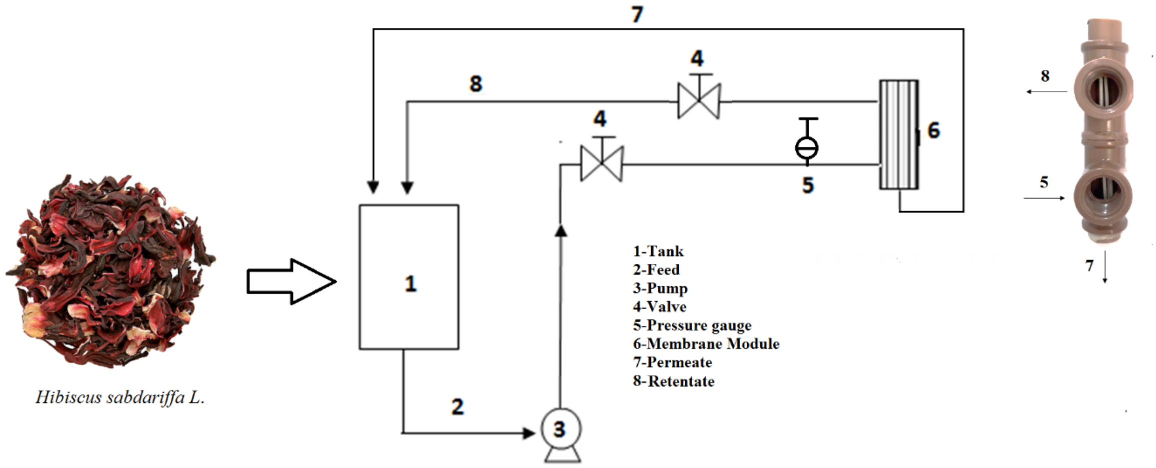

Fig. 1 Experimental unit for cross-flow filtrations of hibiscus extracts through spinel hollow fiber membranes

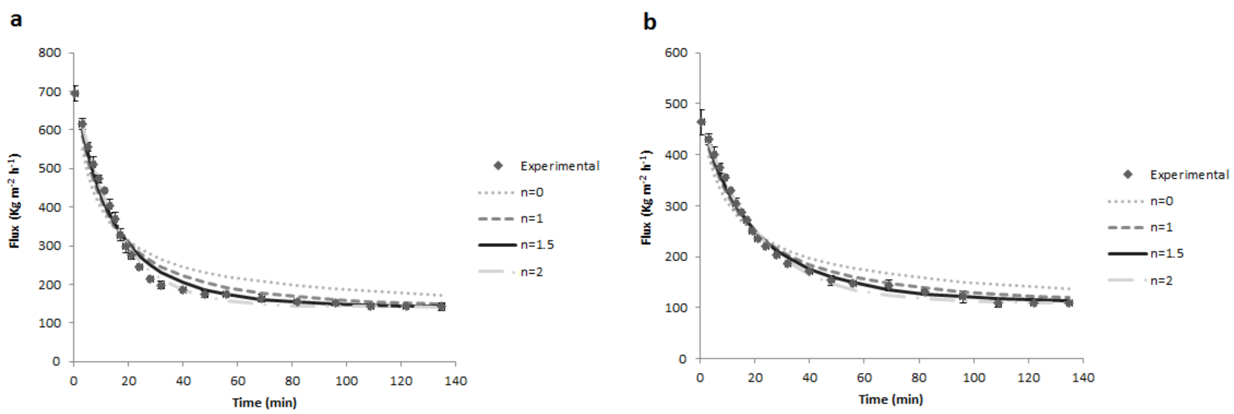

Fig. 2 Experimental and calculated flux data for hibiscus extract by Field et al. (1995). With pretreatment (a) and without pretreatment (b). Cake formation (n = 0), partial pore block (n = 1), internal pore block (n = 1.5) and complete pore block (n = 2)

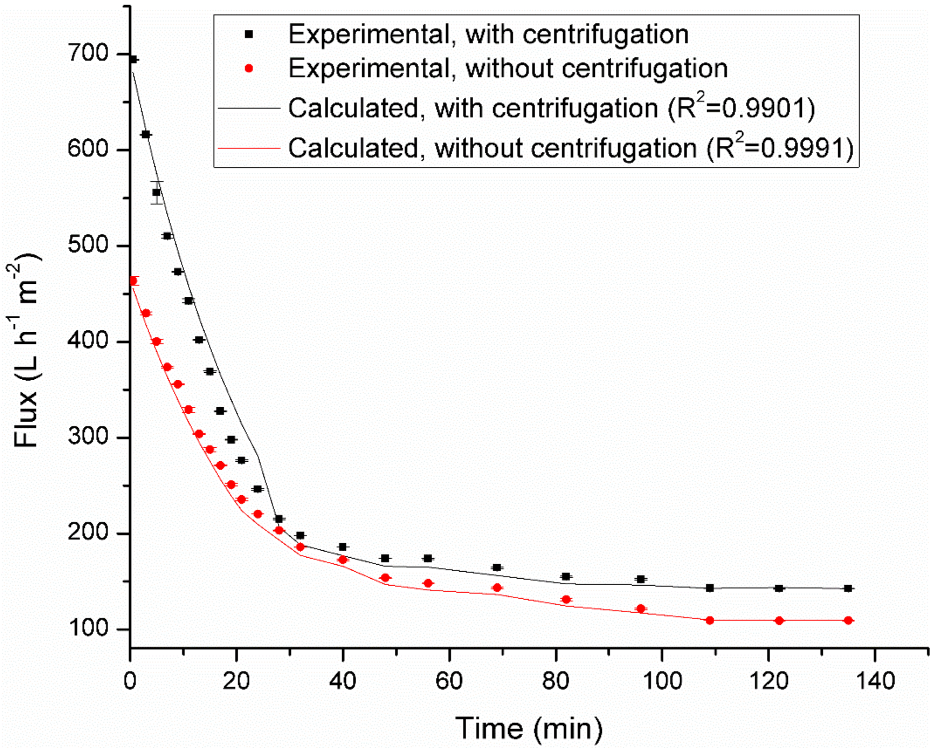

Fig. 3 Experimental and calculated (Mondal & De, 2009) flux decays for membrane filtrations of centrifuged and non-centrifuged hibiscus extracts

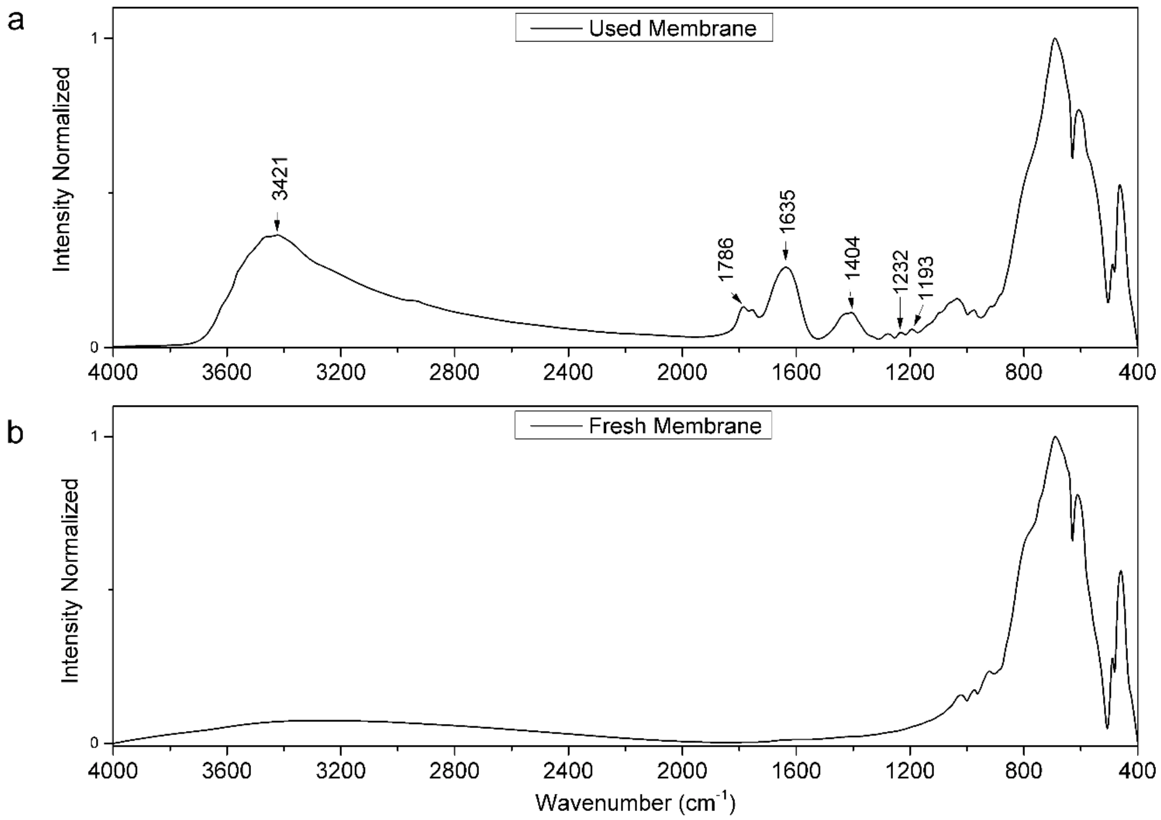

Fig. 4 Fourier infrared spectra of used and fresh membranes

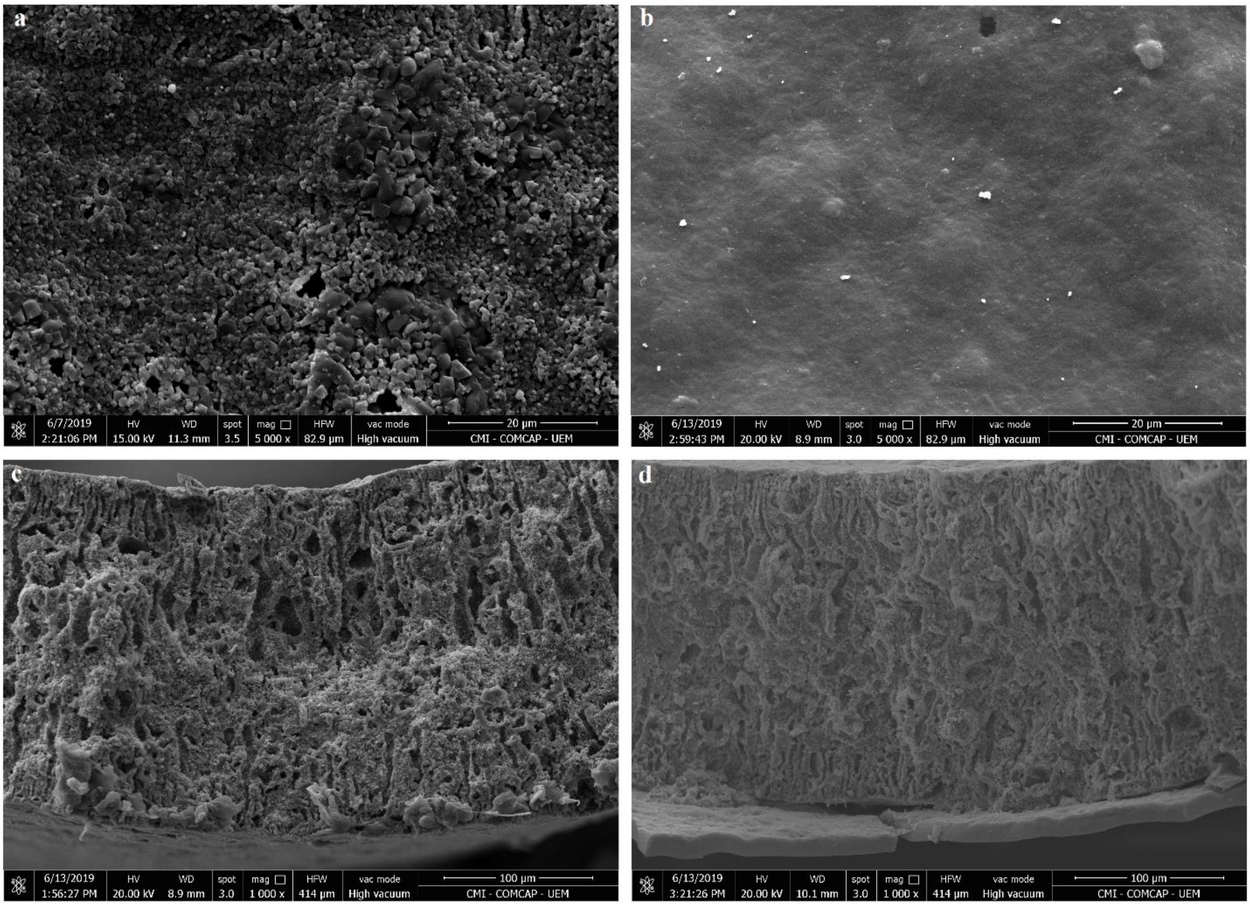

Fig. 5 Images of asymmetric hollow fiber membranes. Outer surface before extract filtration (a), Outer surface after extract filtration (b), Cross-sectional view before extract filtration (c) and Cross-sectional view after extract filtration (d)

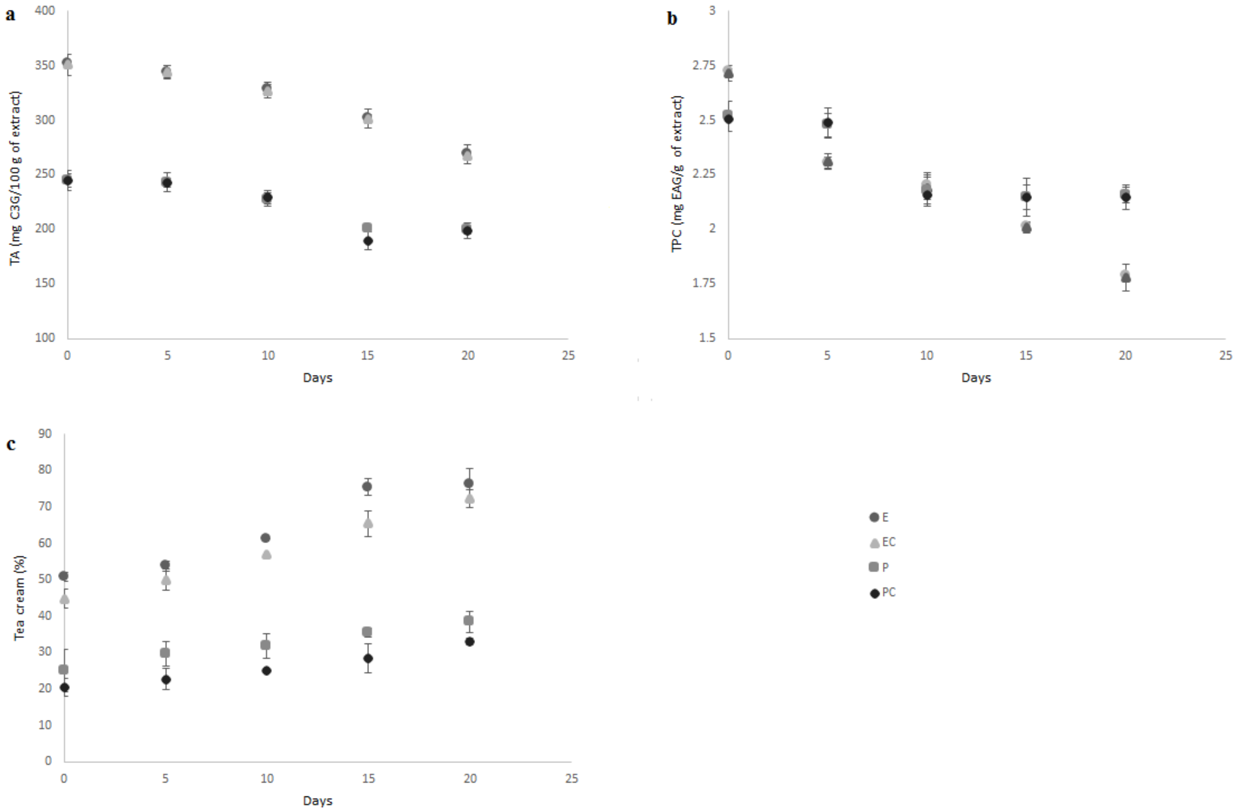

Fig. 6 Extract and permeate stability. Anthocyanins (a), Phenolic Compounds (b) and Tea cream (c) within 20 days of storage

ARTIGO 2

Investigation of techniques to mitigate membrane fouling in cross-flow ultrafiltration of hibiscus (*Hibiscus sabdariffa L.*) extract

Carolina Moser Paraíso[a], Jessica dos Santos Pizzo[b], Mariana Sversut Gibin[c], Eduardo Azzolini Volnistem[c], Jesuí V. Visentainer[b], Francielle Sato[c], Silvio Cláudio da Costa[d], Miria Hespanhol Miranda Reis[e], Grasiele Scaramal Madrona[f]

[a]Graduate Program in Food Science, State University of Maringá, Avenida Colombo 5790, Maringá-PR, Brazil. *carolina.moser@hotmail.com

[b]Department of Chemistry, State University of Maringá, Avenida Colombo 5790, Maringá-PR, Brazil.

[c]Department of Physics, State University of Maringá, Avenida Colombo 5790, Maringá-PR, Brazil.

[d]Department of Biochemistry, State University of Maringá, Avenida Colombo 5790, Maringá-PR, Brazil.

[e] Faculty of Chemical Engineering, Federal University of Uberlândia, Av. João Naves de Ávila, 2121, Uberlândia-MG, Brazil

[f] Department of Food Engineering, State University of Maringá, Avenida Colombo 5790, Maringá-PR, Brazil.

Abstract

This study evaluated the application of different techniques (turbulence promoter, ultrasound-assisted, and turbulence promoter plus ultrasound) to mitigate fouling during filtration of hibiscus extract. The use of ultrasound, turbulence promoter and turbulence promoter plus ultrasound increased the flux by 21, 44 and 88%, respectively. Pore

blockage was the main mechanism of fouling and polysaccharides, proteins and phenolic compounds were most likely responsible for membrane fouling as shown by Fourier-transform infrared spectroscopy. Analysis of atomic force microscopy showed that compared with the roughness of the virgin membrane, the control membrane was 12 times larger and the membrane with turbulence plus ultrasound was only 2 times larger. The use of a turbulence promoter plus ultrasound did not alter the hibiscus extract quality and retention greater than 60% was observed for total phenolic compounds, total anthocyanins, cyanidin-3-glucoside, delphinidin, quercetin, myricetin, and rutin. Overall, the combination of turbulence promoter and ultrasound in the ultrafiltration module shows great potential to significantly mitigate membrane fouling and improve cross-flow filtration.

Keywords: Turbulence promoter, Ultrasound, Membrane filtration, Flux modeling.

1. Introduction

Hibiscus sabdariffa L., also known as roselle or hibiscus, is an annual medicinal shrub of the genus *Hibiscus* of the *Malvaceae* family, being widely cultivated in tropical and subtropical environments. The main economic interest of hibiscus is its calyces, mainly used for the elaboration of hot infusions and cold drinks, and recently they have been investigated for therapeutic potential (Da-costa-rocha et al., 2014; Guardiola & Mach, 2014). Hibiscus calyces have a high content of bioactive compounds, mainly anthocyanins and other phenolic compounds responsible for its antioxidant (Cid-Ortega & Guerrero-Beltrán, 2015; Da-costa-rocha et al., 2014). Scientific studies have reported pharmacological properties of dry calyx extract including strong antihypercholesterolaemic, antihypertensive, antinociceptive, antipyretic effects, among others (Pinela et al., 2019; Riaz & Chopra, 2018).

The membrane filtration process is a constantly evolving technology in the food industry and with many applications in plant extract processing, mainly due to the preservation of bioactive compounds. This process is carried out at room temperature, with minimum energy demand, which is quite interesting since these compounds are thermosensitive (Bindes et al., 2019; Madrona et al., 2018). Several recent studies have reported the efficacy of this method in the processing of plant extracts for recovery, purification and concentration of bioactive compounds, as in uvaia (Rodrigues et al., 2021), pequi (Magalhães et al., 2019), and camu-camu residue (Rodrigues et al., 2020) among others.

One of the disadvantages in the membrane separation is the fouling occurrence, resulting from the deposits formed by the components of the filtered material that accumulate on the surface or pores of the membrane. This deposit can result in a significant loss in permeate flux, thus reducing filtration efficiency (Kelly et al., 2019). In addition, severe membrane fouling can increase operating time, cost (cleaning, maintenance and energy), decrease membrane life and deteriorate extract or juice quality. Thus, it is essential to understand the mechanisms of membrane fouling and to provide solutions to this problem (Lu et al., 2021; Castro-Muñoz, 2018).

A promising technique for reducing membrane fouling during filtration is the use of turbulence promoters. These devices induce shear rates that increase turbulence on the membrane surface, promoting reduction of solutes and particles deposition. Turbulence promoters made from 3D printing are a viable alternative due to low cost and energy for production, variety of materials and the ability to create different geometric shapes (Tsai et al., 2019). Ferreira et al. (2020) showed that 3D cylindrical promoters of turbulence used in ultrafiltration of araça extract increased the permeate flux by up to 78%.

Another alternative that can be used for fouling mitigation is ultrasound-assisted filtration. This method uses the energy of sound waves that propagate in the medium creating cycles of compression and expansion, causing the molecules to move away and approach several times (Córdova et al., 2020). This process of compression and expansion produces the phenomenon called cavitation, which consists of the production, growth and collapse of bubbles. The asymmetric collapse of the bubbles generates microjets resulting in zones of high shear energy and turbulence in the deposit layer that forms on the membrane's surface (Cassano et al., 2011). Recent studies with green tea (Sousa et al., 2016) and jenipapo extract (Madrona et al., 2018) used ultrassound in the clarification process and proved that the reduction of membrane fouling increasing thus the permeate flux.

As an innovative factor this study presented a combination of techniques to reduce fouling during membrane filtration of hibiscus. According to previous work, turbulence promoters and ultrasound can improve the performance of membrane filtration of food fluids (Ferreira et al., 2020; Sousa et al., 2016), but the effects of combining these techniques has not yet been investigated.

In this context, the present work aimed: i) to evaluate the application of turbulence promoter, ultrasound-assisted, and turbulence promoter plus ultrasound in hibiscus extract filtration, ii) to determine the modeling of permeate flux and calculate the resistance to systematically investigate the fouling process, and iii) to evaluate physicochemical analyzes of extracts and permeates.

2. Material and Methods

2.1 Chemicals and reagents

6-hydroxy-2,5,7,8-tetramethylchromane-2-carboxylic acid (Trolox), 2,2-diphenyl-1-picrylhydrazyl (DPPH), Folin reagent, Calcium gallate, were obtained from Sigma-Aldrich Chemical Co. (St. Louis, MO, USA). Cyanidin 3- glucoside, ellagic acid, gallic acid, rutin, quercetin, p-coumaric acid, myricetin and delphinidin chloride were the standards also used from Sigma-Aldrich. Methanol (chromatography grade) was purchased from J. T. Baker (Edo. de Mexico, Mexico). Ultrapure water was obtained from a Milli-Q ultrapure water purification system (Millipore, USA). Formic acid (chromatography grade) was purchased from Sigma-Aldrich (Saint Louis, USA). All other reagents used were of analytical grade.

2.2 Ultrafiltration of hibiscus calyx extract

Hibiscus calyces were purchased in October 2020 in the local commerce (Maringá, Paraná-Brazil). The calyces were crushed and classified according to granulometry using Tyler sieves. To obtain the aqueous hibiscus extract, the samples (particle size of 0.420 - 0.595 mm) were inserted in an ultrasonic bath (Ultracleaner 1650 Unique, frequency of 40 KHz) at 60°C for 45 minutes and the calyx:solvent ratio of 1:10, using distilled water as solvent (Paraíso et al., 2019) The extract was centrifuged at 8000 rpm for 20 min and filtered on filter paper under vacuum to remove rough particles.

In the cross-flow filtration unit (Figure 1A), the flat polyethersulfone membrane (Microdyn-Nadir®) of 5 kDa with a membrane filtration area of 6.36 x 10^{-3} m^2 was evaluated. A pump with half its rotation (2.4 L/min) was used. The filtrations were performed at room temperature (approximately 25 ° C) and at 10 bar of pressure. The retained and permeate flux were returned to the feed tank (total recycling mode). Filtrations were carried out to a concentration factor of 2. After the filtration process started, samples were collected throughout the process to measure flux behavior as a function of filtration time, the flux was calculated using Equation 1.

$$J = \frac{m}{At} \tag{1}$$

where J is the permeate flux (Kg m^{-2} $h^{-1)}$, m is the mass of the permeate (Kg) and t is the time interval to collect the permeate samples (h).

To increase the permeate flux, filtration with turbulence promoter, ultrasound-assisted, and turbulence promoter plus ultrasound (named promoter+ultrasound) were evaluated. The change in volumetric flux over time with the use of these techniques was compared with that of conventional filtration (named control). For promotor filtration, a turbulence promoter was used that was coupled to the planar filtration module and used in the tangential configuration. The turbulence promoter was produced in a 3D printer (Sethi S2) using 3Dla's flexible filament and was designed with 108 pin., 6 mm spacing between the pins, 2.5 mm of internal diameter, and 1.8 mm of height (Figure 1B) (Ferreira et al., 2020). For ultrasound filtration, the module with the membrane was inserted into the ultrasound device (Ultracleaner 1650 Unique,frequency of 40 KHz), and it was switched on from the beginning of filtration.

2.3 Mathematical Modeling

To determine decay of the permeated flux during cross-flow filtration with constant pressure, the mathematical model proposed by Field et al. (1995) was used (Equation 2).

$$-\frac{dJ}{dt}J^{n-2} = K(J - J^{*}) \tag{2}$$

where J is the permeate flux (Kg h^{-1} m^{2}), J^{*} *is* the critical flux (Kg h^{-1} m^{2}), t is the filtration time (h), K is the adjusted parameter and n is the exponent that indicates the fouling mechanism that occurs during the membrane filtration process (cake formation n=0, complete pore blockage n=2, intermediate pore blockage n=1 and internal pore blockage n=1.5). For each value of "n" Equation 5 was solved numerically using the Levenberg-Marquardt method in the Fortran program using an integration step of 10^{-3} with accuracy of $10^{-8.}$ The calculated flux profiles were compared with such experiment flux data. To verify the main fouling mechanism during the filtration of hibiscus extract, the values of R^2 were determined between numerical calculations and experimental data.

The membrane resistances were calculated based on the serial resistance model to describe fouling during filtration. Total resistance (R_T) was determined from the sum of the hydraulic membrane resistance (R_M), cake resistance (R_C) and pore blockage resistance (R_P). The hydraulic membrane resistance was determined from the flux of distilled water in a virgin membrane, as presented in Equation 3.

$$R_M = \frac{\Delta P}{J_{W0}\eta} \tag{3}$$

where R_M is the membrane resistance (m^{-1}), J_{W0} is the flux of water through a new membrane ($m\ s^{-1}$)' ΔP is the transmembrane pressure (Pa) and η is the dynamic viscosity of water (Pa s).

After the hibiscus filtration, the flux of distilled water was again determined to obtain resistance due to cake formation and pore blockage, according to Equation 4.

$$R_P + R_C = \frac{\Delta P}{\eta J_{W1}} \tag{4}$$

where R_p is resistance due to pore blockage (m^{-1}), R_c is resistance due to cake formation (m^{-1}), ΔP is transmembrane pressure (Pa), η is the dynamic viscosity of water (Pa s) and J_{W1} is the flux of water through the membrane used ($m\ s^{-1}$).

After gently removing the cake layer from the membrane surface with a sponge, the resistance due to pore blockage was determined again by the flux of distilled water, as presented in Equation 5.

$$R_P = \frac{\Delta P}{\eta J_{W2}} \qquad (5)$$

Where R_p is the resistance due to pore blockage (m^{-1}), ΔP is transmembrane pressure (Pa), η is the dynamic viscosity of water (Pa s) and J_{W2} is the flux of water through the membrane used after cake removal ($m\ s^{-1}$).

2.4 Membrane characterization

After the filtration process the control membrane, the virgin membrane and the promoter+ultrasound membrane were maintained for 24h in a desiccator before instrumental characterization:

Fourier Transform Infrared Spectroscopy: The membrane surfaces were evaluated via Fourier Transform Infrared Spectroscopy (FTIR) on a Vertex 70v FTIR (Bruker Optik GmbH, Ettilingen, DEU) spectrometer equipped with the total attenuated reflectance accessory (ATR) equipped with diamond crystal (Bruker Optik GmbH, Ettilingen, DEU) (FTIR-ATR). The spectra were obtained from 4000 to 400 cm^{-1} with a spectral resolution of 4cm^{-1}, each spectrum being an average of 128 scans, collected at a temperature of 25 °C.

Fourier transform infrared microspectroscopy with total attenuated reflection (μATR-FTIR): The surfaces of the control membrane and the promoter+ultrasound were mapped by an FTIR microscope model Lumos II (Bruker Optik GmbH, Ettilingen, DEU) operated in total attenuated reflection mode (ATR), equipped with germanium crystal and motorized platform to obtain the spectra in the predefined positions. The spectra were obtained in a matrix of 13x13 and the product of 100 scans, in a spectral range of 4000 to 750 cm^{-1}, spatial resolution of 4 cm^{-1} and opening of 100x100µm, collected at room temperature of 25ºC. Data were processed equally for both membranes using the software OPUS version 8.5 (Bruker Optik GmbH, Ettilingen, DEU).

Atomic force microscopy: Atomic force microscopy (AFM) images were obtained using a Shimadzu atomic force microscope (SPM-9700) with a Si tip, with a spring constant 0.5-9.5 N/m and of resonance frequency 4.5-9.5 kHz, by using dynamic (tapping) mode. The root-mean-squared (RMS) roughness (Rq) of membranes was calculated from 10x10 µm height images using the Gwyddion software.

2.5 Hibiscus extract characterization

The extract and permeates of the control and of the promoter+ultrasound were analyzed for pH, total soluble solids (TSS), total solids (TS), total phenolic compounds (TPC), total anthocyanins (TA), antioxidant activity (AA) and instrumental color.

The pH values were determined in a digital pHmeter (PG2000) and the soluble solids content (°Brix), by using a digital refractometer (HI 96801 Hanna). The total solids content was determined by weighing 5 mL of the sample before and after drying in an oven at 103-105 °C for 24h (AOAC, 2016).

The total phenolic compounds content (TPC) was quantified by the Folin-Ciocalteu method using a standard gallic acid curve (R^2=0.99) and the absorption measured in 725 (UVmini - 1240 Shimadzu) (Pierpoint, 2004; Singleton & Rossi, 1965). The results were expressed in mg of gallic acid equivalent (GAE) g^{-1} of extract. The total anthocyanin content (TA) was quantified by the single pH method (pH=1) and the absorbance at 535 nm (UVmini – 1240 Shimadzu) (Lees & Francis, 1972). Total anthocyanins were expressed in mg equivalent of cyanidin-3-glucoside (C3G).100 g^{-1} extract.

Antioxidant activity (AA) was determined by the ability of antioxidants present in the samples to be used to register the stable radical DPPH (2,2-diphenyl-1-picrilhydrazil). The radical reduction was determined according to the methodology described by Thaipong et al. (2006). Absorbance was measured at 515 nm (Shimadzu, model UVmini – 1240) and antioxidant activity was calculated from the standard Trolox curve (R2 = 0.99) and expressed in mM Trolox extract (TE) g^{-1}.

Color was evaluated using the portable colorimeter Minolta® CR400, using Ciel*a*b*system, in which the coordinates were measured: L, representing the luminosity on a scale from 0 (black) to 100 (white); a* representing a tonality scale ranging from red (0 + a) to green (0 - a) and b* representing a scale from yellow (0 + b) to blue (0 - b).

Ultra performance liquid chromatography - mass spectrometer (UPLC-MS/ MS) analyses were done as reported previously by Barizão et al. (2013) and Lopes et al. (2018). Briefly, the bioactive compounds of hibiscus extract and permeates were identified and quantified using a Waters ACQUITY UPLC® H-Class System (Miliford, MA, USA) coupled to a Xevo TQD triple-quadrupole mass spectrometer equipped with a Z spray™ electrospray ionization (ESI) source (Waters, Milford, MA, USA). For chromatographic separation of bioactive compounds, the extracts were injected into an Acquity UPLC® BEH C18 column (50 × 2.1 mm (i.d.), 1.7 μm particle size) (Waters, Milford, MA, USA) that was kept at 40 ± 1 °C. The mobile phases were water acidified with 0.1% formic acid (solvent A) and methanol (solvent B) at a flux rate of 0.300 mL min^{-1}. The ESI source was operated in positive and negative ion mode using the following MS/MS parameters: 3.0 kV in positive and -2.5 kV in negative ion mode for the capillary voltage, 3.0 V extractor voltage, 150 °C source temperature and 550 °C desolvation gas temperature. Nitrogen was used both as the desolvation gas and the cone gas, with flux rates set at 800 and 50 L h^{-1}, respectively. The collision gas (99.9% argon from White Martins, Rio de Janeiro, Brazil) was set at a pressure of 3.00×10^{-3} mbar. For the quantification of samples extract [methanol:water (50:50, v/v)], analytical curves were constructed at six concentration levels in triplicate. Results were expressed as mg g^{-1} of extract.

2.6 Statistical analysis

Analyzes were performed in triplicate and were statistically evaluated by analysis of variance (ANOVA), compared by the Tukey test with a significance level of 5% ($p \leq 0.05$) using the Sisvar 5.6 statistical program.

3. Results and Discussion

3.1 Flux analyses for hibiscus extract filtrations

Figure 2 shows the permeate flux as a function of time during the hibiscus extract ultrafiltrations through a 5 kDa membrane at 10 bar. A marked decay in permeate fluxes was observed in the first 10 min, followed by a stabilization period. The decreasing trend in permeate flux can be attributed to factors such as small pore diameters and intrinsic membrane resistance (Qin et al., 2015). Similar permeate fluxes behaviors were observed in membranes for pequi extract (de Santana Magalhães et al., 2019) and yerba mate extract (Gerke et al., 2017).

Compared to control filtration (named control), the use of ultrasound, turbulence promoter, and promoter+ultrasound increased the initial flux by 21, 44 and 88%, respectively. The significant flux increase with the use of promoter+ultrasound may be due to the promoter that when applied in membrane filtration increases the shear tension on the membrane surface attenuating fouling (Tsai et al., 2019). In addition, application of ultrasonic energy in the process can increase the flux by breaking the cake layer on the membrane surface due to vibration caused by the ultrasound frequency (Córdova et al., 2020). A recent study evaluated the microfiltration of artificial seawater using three promoters of turbulence with different 3D configurations (circular, diamond and elliptical) and reported that the elliptical promoter was the most efficient, increasing the flux by approximately 30-64% under a transmembrane pressure of 20 kPa compared to conventional microfiltration (Tsai et al., 2019). Popović and Tekić (2011) tape turbulence promoters on milk microfiltration and observed that the tighter twisted tape showed a significant increase in flux.

In relation to the stabilized flux, there was also a significant improvement, and the fluxes were 97.55, 155.28, 205.99 and 367.61 Kg/hm^2, for control filtration, ultrasound, turbulence promoter, and promoter+ultrasound, respectively. A recent study evaluated the application of a 50 kDa membrane in ultrasound-assisted ultrafiltration for the purification of phenolic compounds from jenipapo extract and observed up to 80% improvement in the stabilized flux (Madrona et al., 2018).

Figure 3 shows the visual appearance of membranes after hibiscus extract filtration. The control filtration (Figure 3A) presented the highest cake formation, and the membrane surface was covered by a continuous layer of particles. The filtration with promoter+ultrasound (Figure 3D) had the membrane with lowest particle deposition, corroborating the experimental data of the permeate flux (Figure 2). This combination has great potential to significantly mitigate membrane fouling and improve flux in ultrafiltration processes.

Experimental cross-flow data in ultrafiltration membranes were adjusted according to the decay flux model proposed by Field et al. (1995) for each fouling mechanism. Correlating the data of experimental and calculated fluxes according to the filtration time (Figure 2A-2D), all scale mechanisms contributed to flux decay in the initial stages of filtration. As shown in Table 1, the predominant overall fouling mechanism for control filtration was internal pore blockage (R^2=0.996), for filtration with ultrasound was internal pore blockage (R^2=0.997) and complete pore blockage (R^2=0.997), for filtration with turbulence promoter was internal pore blockage (R^2= 0.993) and complete pore blockage (R^2=0.993), and for filtration with promoter+ultrasound it was partial pore blockage (R^2=0.991). For all filtration processes, the flux profile has not been well described by cake formation possibly because the molecular weight of various hibiscus extract components is smaller than the size of the membrane pores. In addition, the extract has a high solids content and can form cake in the first minutes of filtration and after that the particles are deposited in the pores due to the high pressure used in the process (Sousa et al., 2016).

A similar study evaluated the filtration process through asymmetric ceramic hollow membrane for clarification of hibiscus extract and observed that the predominant global fouling mechanism was complete pore blockage (Paraíso et al., 2020). Li et al. (2018) evaluated 19-channel zirconia ceramic ultrafiltration membrane with an average pore size of 0.05 μm for clarification of heated sugarcane juice broth and observed that the mechanism of flux reduction during ultrafiltration was the formation of cake on the membrane surface. These results suggest that the fouling mechanisms during filtration depend on the interactions between the membrane and the solutes in the extract, pore size and membrane material, as well as operating parameters and solute nature (Balyan et al., 2019; Cassano et al., 2017).

Resistance due to cake formation (R_C) is responsible for approximately 40% of the total filtration resistance (Table 2). Similarly, Ennouri et al. (2015) observed that in the total recycling mode in the pomegranate juice filtration, the resistance due to cake formation was 52.6%. Compared to control filtration, the use of ultrasound, turbulence promoter and promoter+ultrasound, reduced the total resistance (R_T) by 11, 31 and 38%, respectively.

Considering that the ultrafiltration of hibiscus extract using promoter+ultrasound presented the best permeate flux, it was chosen for the next steps (characterization).

3.2 Membrane characterization

The virgin membrane (Figure 4) presents several vibrational modes due to the long chains present in the polymer, being detectable in the control and in the promoter+ultrasound membrane (identified by asterisk). The band referring to the presence of the hydroxyl group (O-H stretch), region of 3,080 – 3,540 cm^{-1} is extended in the control membrane and in the promoter+ultrasound membrane, evidencing a shoulder ~3,360 cm^{-1}, possibly due to the stretch modes of NH_2, overlapped with the hydroxyl group (Lee et al., 2013; Paraíso et al., 2020). Carbonyls were detected by Paraíso et al. (2020) in hibiscus extracts and are present in the spectra at 1,787 and 1,737 cm^{-1}, stretch of C=O, which may come from carboxylic acid and ester/aldehyde, respectively (Pappas et al., 1998; Socrates, 2001). The promoter+ultrasound membrane shows a band at 1,620 cm^{-1}, while the control membrane is at 1,608 cm^{-}1. The region of 1,600 to 1,700 cm^{-1} is characteristic of vibrational modes of amide I, directly associated with proteins, being: C=O stretch with contribution of C-N and N-H (Luján-Facundo et al., 2015). Furthermore, the control membrane has a band at 1,224 cm^{-1} referring to C-O deformation, with the region of 1,540 to 1,175 cm^{-1} being attributed to flavonols and phenols (Luján-Facundo et al., 2015; Tahir et al., 2017). Patle et al. (2020), specifies the region, from 1,260 to 1,200 cm^{-1}, as C-O-C of the ester for quercetin. Both encrusted membranes have C-O stretch vibration modes at 956 cm^{-1}, associated with polysaccharide retention (Choong et al., 2019; Liu, 2013). The results point to proteins, bioactive compounds and polysaccharides as being the causative agents of membrane fouling. A previous study also observed the presence of molecules such as polysaccharides, proteins and phenolic compounds by FTIR analysis after ultrafiltration of sugarcane juice in a 19-channel ceramic membrane (Li et al., 2018).

Figure 5 displays the surface of the control and the promoter+ultrasound membrane after filtration of hibiscus extract, which were mapped using the FTIR-μATR. The membrane-associated band was integrated to obtain the corresponding contour maps in Figure 5. The promoter+ultrasound membrane (Figure 5A) presents maximum area in 0.8 and regions between 0.2 and 0.4. While the control membrane (Figure 5B) has a maximum area in 0.4 with regions between 0 and 0.2. Therefore, promoter+ultrasound incrusted less material since the membrane is more evident in this mapping when compared to the control membrane.

The three-dimensional morphological characteristics of the surfaces of the virgin and incrusted membrane were characterized by AFM to observe the fouling after extract filtration (Figure 6). Figures 6A and 6B show that the virgin membrane presented roughness and irregular surface, which is characterized by the typical "peak-valley" morphology (Vieira et al., 2018). According to Li et al. (2018) in the initial period of filtration, especially in the first 10 min, particles accumulate in the valley of the membranes, resulting in the rapid flux decline, corroborating the flux data of Figure 2.

For a quantitative analysis, the mean square roughness of the surface was calculated in the first part of the area presented in Figure 6. Roughness analysis has been used as a good indicator of the performance of polymer membranes and widely applied in other studies (Boussu et al., 2005; Carvalho et al., 2011; Izák et al., 2008). The roughness values were 12.55 nm ± 1.2, 151.3 nm ± 12.3, 30.25 nm ± 8.7, for the virgin membrane, control membrane and promoter+ultrasound membrane respectively. Thus, in the post processes of filtration of hibiscus extract, a significant increase in roughness was observed in relation to the virgin membrane, due to the deposition of solute on the surface of the membrane (Rabelo et al., 2016). In addition, it can be observed that when compared with the roughness of the virgin membrane, the control membrane was 12 times larger and the promoter+ultrasound membrane was only 2 times larger, confirming the results (Figure 2) that the association of these methods has great potential to significantly mitigate blockage and improve cross-flow.

3.3 Physicochemical analyses of extracts

The membrane filtration process resulted in significant changes for all parameters evaluated (Table 3). However, the use of promoter+ultrasound did not alter the hibiscus extract quality. A previous study also reported that the use of 3D turbulence promoter in flat membranes of 10 kDa did not alter the characteristics of araçá roxo extract (Ferreira et al., 2020).

After membrane filtration there was a slight increase in the pH value. In addition, there was a reduction of 45% and 51% for TS and TSS, which is very significant. Similarly, Cassano et al. (2019) observed a significant reduction in TS and TSS content after filtration of aqueous extract from red wine lees in nanofiltration flat configuration membranes.

Membrane filtration increased the L* values of hibiscus extract, possibly due to anthocyanin retention by the ultrafiltration membrane. Thus, the permeates had less color with higher luminosity (Figure 7). This behavior was also observed in the concentration of jussara ethanol extract using nanofiltration membranes (Vieira et al., 2018). In relation to parameters a* and b* there was also an increase after filtration. This result corroborates a previous study that used ultrasound-assisted membrane filtration for the treatment of jenipapo extract with an ultrafiltration membrane of 50 kDa (Madrona et al., 2018).

In relation to the bioactive compounds analyzed, a retention greater than 60% was observed for total phenolic compounds, total anthocyanins, cyanidin-3-glucoside, delphinidin, quercetin, myricetin and rutin. The high retention of hibiscus bioactive compounds after ultrafiltration suggests the potential for the application of 5 kDa membrane to produce concentrated extract with functional properties. Conidi et al. (2017) observed that the retention of anthocyanins in pomegrate juice was 66-99% in 4 kDa polyethersulfone membrane. Cissé et al. (2018) reported that for a 5 kDa polyethersulfone membrane the retention of total anthocyanins varied between 93% and 97% when the transmembrane pressure increased from 1 to 3 MPa. The retention of bioactive compounds in membrane filtration is not directly related to the molecular weight of the membrane cut, and the bioactive compounds are much smaller than the average size of the pores of the membrane used. Therefore, possibly the retention of bioactive compounds by ultrafiltration can be attributed to the formation of a dynamic layer on the membrane surface and/ or interactions between bioactive compounds and other components present in the extract forming particles (Cassano et al., 2017; Sousa et al., 2016). Comparing p-coumaric with other compounds, p-coumaric has the lowest molecular weight (163.0 g/mol), and therefore completely passed through the ultrafiltration membrane. Similar behavior for the p-coumaric molecule was observed in the clarification and concentration of pequi fruit extract by sequential membrane filtration (de Santana Magalhães et al., 2019).

In order to evaluate the effects of membrane filtration on the antioxidant activity of hibiscus extract, the DPPH assay was used. The membrane filtration process caused reductions in DPPH values, but the extract still maintained its antioxidant property after filtrations. Similarly, Seifzadeh et al. (2019) reports a significant reduction in antioxidant activity in pistachio hull permeate after 10 kDa membrane filtration.

4. Conclusion

The application of ultrasound, turbulence promoter and the association of these two methods resulted in higher permeate flux for hibiscus extract (88 % higher than the control). The mathematical modeling of flux decay during ultrafiltration shows that pore blockage was the main mechanism of fouling and polisaccharides, proteins and bioactive compounds were most likely responsible for fouling as observed by FTIR.

The use of a turbulence promoter+ultrasound did not alter the hibiscus extract quality, highlighting the retention greater than 60% was observed for total phenolic compounds, total anthocyanins, cyanidin-3-glucoside, delphinidin, quercetin, myricetin, and rutin. Thus, the combination of promoter+ultrasound in the ultrafiltration module shows great potential to significantly mitigate membrane fouling and improve cross-flow filtration.

References

AOAC. (2016). Official Methods of Analysis, 20th edition. *Association of Official Analytical Chemists*.

Balyan, U., Verma, S. P. & Sarkar, B. (2019). Phenolic compounds from Syzygium cumini (L.) Skeels leaves: Extraction and membrane purification. *Journal of Applied Research on Medicinal and Aromatic Plants, 12,* 43–58. https://doi.org/10.1016/j.jarmap.2018.12.002

Barizão, É. O., Martins, A. C., Ercoli, L., Kvitschal, M. V., Silva, R., Pezoti Junior, O., Visentainer, J. V. & de Cinque Almeida, V. (2013). Optimization of Antioxidant Compounds Extraction from Flesh of New Developed Apple Cultivar Using Response Surface Methodology. *Food Analytical Methods*, *6*(5), 1407–1415. https://doi.org/10.1007/S12161-012-9558-4

Bindes, M. M. M., Cardoso, V. L., Reis, M. H. M. & Boffito, D. C. (2019). Maximisation of the polyphenols extraction yield from green tea leaves and sequential clarification. *Journal of Food Engineering*, *241*, 97–104. https://doi.org/10.1016/j.jfoodeng.2018.08.006

Boussu, K., Van Der Bruggen, B., Volodin, A., Snauwaert, J., Van Haesendonck, C. & Vandecasteele, C. (2005). Roughness and hydrophobicity studies of nanofiltration membranes using different modes of AFM. *Journal of Colloid and Interface Science*, *286*(2), 632–638. https://doi.org/10.1016/J.JCIS.2005.01.095

Carvalho, A. L., Maugeri, F., Silva, V., Hernández, A., Palacio, L. & Pradanos, P. (2011). AFM analysis of the surface of nanoporous membranes: application to the nanofiltration of potassium clavulanate. *Journal of Materials Science*, *46*(10), 3356–3369. https://doi.org/10.1007/S10853-010-5224-7

Cassano, A., Bentivenga, A., Conidi, C., Galiano, F., Saoncella, O. & Figoli, A. (2019). Membrane-Based Clarification and Fraction of Red Wine Lees Aqueous Extracts. *Polymers*, *11*(7), 1089. https://doi.org/10.3390/polym11071089

Cassano, A., Conidi, C. & Drioli, E. (2011). Clarification and concentration of pomegranate juice (Punica granatum L.) using membrane processes. *Journal of Food Engineering*, *107*(3–4), 366–373. https://doi.org/10.1016/j.jfoodeng.2011.07.002

Cassano, A., De Luca, G., Conidi, C. & Drioli, E. (2017). Effect of polyphenols-membrane interactions on the performance of membrane-based processes. A review. *Coordination Chemistry Reviews, 351,* 45–75. https://doi.org/10.1016/j.ccr.2017.06.013

Castro-Muñoz. (2018). Separation, Fractionation and Concentration of High-Added-Value Compounds From Agro-Food By-Products Through Membrane-Based Technologies. *Encyclopedia of Food Security and Sustainability*, *1*, 465–476. https://doi.org/10.1016/B978-0-08-100596-5.22282-8

Choong, Y.-K., Mohd Yousof, N. S. A., Jamal, J. A. & Isa Wasiman, M. (2019). Determination of anthocyanin content in two varieties of Hibiscus Sabdariffa from Selangor, Malaysia using a combination of chromatography and spectroscopy. *Journal of Plant Science and Phytopathology*, *3*(2), 067–075. https://doi.org/10.29328/JOURNAL.JPSP.1001034

Cid-Ortega, S. & Guerrero-Beltrán, J. A. (2015). Roselle calyces (Hibiscus sabdariffa), an alternative to the food and beverages industries : a review. *Journal of Food Science and Technology*, *52*, 6859–6869. https://doi.org/10.1007/s13197-015-1800-9

Cissé, M., Vaillant, F., Pallet, D. & Dornier, M. (2018). Selecting ultrafiltration and nanofiltration membranes to concentrate anthocyanins from roselle extract (Hibiscus sabdariffa L.). *Food Research International*, *44*(9), 2607–2614. https://doi.org/10.1016/j.foodres.2011.04.046

Conidi, C., Cassano, A., Caiazzo, F. & Drioli, E. (2017). Separation and purification of phenolic compounds from pomegranate juice by ultrafiltration and nanofiltration membranes. *Journal of Food Engineering, 195,* 1–13.

https://doi.org/10.1016/j.jfoodeng.2016.09.017

Córdova, A., Astudillo-Castro, C., Ruby-Figueroa, R., Valencia, P. & Soto, C. (2020). Recent advances and perspectives of ultrasound assisted membrane food processing. *Food Research International*, *133*, 109163. https://doi.org/10.1016/j.foodres.2020.109163

Da-costa-rocha, I., Bonnlaender, B., Sievers, H., Pischel, I. & Heinrich, M. (2014). Hibiscus sabdariffa L . – A phytochemical and pharmacological review. *Food Chemistry*, *165*, 424–443. https://doi.org/10.1016/j.foodchem.2014.05.002

de Santana Magalhães, F., de Souza Martins Sá, M., Luiz Cardoso, V. & Hespanhol Miranda Reis, M. (2019). Recovery of phenolic compounds from pequi (Caryocar brasiliense Camb.) fruit extract by membrane filtrations: Comparison of direct and sequential processes. *Journal of Food Engineering*, *257*, 26–33. https://doi.org/10.1016/j.jfoodeng.2019.03.025

Ennouri, M., Ben Hassan, I., Ben Hassen, H., Lafforgue, C., Schmitz, P. & Ayadi, A. (2015). Clarification of purple carrot juice: analysis of the fouling mechanisms and evaluation of the juice quality. *Journal of Food Science and Technology*, *52*(5), 2806–2814. https://doi.org/10.1007/s13197-014-1323-9

Ferreira, F. B., Ullmann, G., Vieira, L. G. M., Cardoso, V. L. & Reis, M. H. M. (2020). Hydrodynamic performance of 3D printed turbulence promoters in cross-flow ultrafiltrations of Psidium myrtoides extract. *Chemical Engineering and Processing - Process Intensification*, *154*, 108005. https://doi.org/10.1016/j.cep.2020.108005

Field, R. W., Wu, D., Howell, J. A. & Gupta, B. B. (1995). Critical flux concept for microfiltration fouling. *Journal of Membrane Science*, *100*(3), 259–272.

https://doi.org/10.1016/0376-7388(94)00265-Z

Gerke, I. B. B., Hamerski, F., Scheer, A. P. & Silva, V. R. (2017). Clarification of crude extract of yerba mate (Ilex paraguariensis) by membrane processes: Analysis of fouling and loss of bioactive compounds. *Food and Bioproducts Processing*, *102*, 204–212. https://doi.org/10.1016/j.fbp.2016.12.008

Guardiola, S. & Mach, N. (2014). Therapeutic potential of Hibiscus sabdariffa : A review of the scientific evidence. *Medicina Intensiva (English Edition)*, *61*(5), 274–295. https://doi.org/10.1016/j.endoen.2014.04.003

Izák, P., Godinho, M. H., Brogueira, P., Figueirinhas, J. L. & Crespo, J. G. (2008). 3D topography design of membranes for enhanced mass transport. *Journal of Membrane Science*, *321*(2), 337–343. https://doi.org/10.1016/J.MEMSCI.2008.05.014

Kelly, N. P., Kelly, A. L. & O'Mahony, J. A. (2019). Strategies for enrichment and purification of polyphenols from fruit-based materials. *Trends in Food Science and Technology*, *83*, 248–258. https://doi.org/10.1016/j.tifs.2018.11.010

Lee, S. V., Vengadaesvaram, B., Arof, A. K. & Abidin, Z. H. Z. (2013). Characterisation of poly (acrylamide-co-acrylic acid) mixed with anthocyanin pigment from hibiscus sabdariffa l . *Pigment & Resin Technology*, *2*, 9420. https://doi.org/10.1108/03699421311301089

Lees, D. H. & Francis, F. J. (1972). Standardization of pigment analyses in cranberries. *Hortscience*, *7*, 83–84.

Li, W., Ling, G., Lei, F., Li, N., Peng, W., Li, K., Lu, H., Hang, F. & Zhang, Y. (2018). Ceramic membrane fouling and cleaning during ultrafiltration of limed sugarne juice. *Separation and Purification Technology*, *190*(1), 9–24. https://doi.org/10.10.1016/j.seppour.2017.08.046

Liu, Y. (2013). Recent Progress in Fourier Transform Infrared (FTIR) Spectroscopy Study of Compositional, Structural and Physical Attributes of Developmental Cotton Fibers. *Materials*, *6*(1), 299–313. https://doi.org/10.3390/MA6010299

Lopes, A. P., Petenuci, M. E., Galuch, M. B., Schneider, V. V. A., Canesin, E. A. & Visentainer, J. V. (2018). Evaluation of effect of different solvent mixtures on the phenolic compound extraction and antioxidant capacity of bitter melon (Momordica charantia). *Chemical Papers*, *72*(11), 2945–2953. https://doi.org/10.1007/S11696-018-0461-3

Lu, C., Bao, Y. & Huang, J. Y. (2021). Fouling in membrane filtration for juice processing. *Current Opinion in Food Science, 42,* 76–85. https://doi.org/10.1016/j.cofs.2021.05.004

Luján-Facundo, M. J., Mendoza-Roca, J. A., Cuartas-Uribe, B. & Álvarez-Blanco, S. (2015). Evaluation of cleaning efficiency of ultrafiltration membranes fouled by BSA using FTIR–ATR as a tool. *Journal of Food Engineering*, *163*, 1–8. https://doi.org/10.1016/J.JFOODENG.2015.04.015

Madrona, G. S., Terra, N. M., Filho, U. C., Santana, F. De, Cardoso, V. L. & Reis, M. H. M. (2018). Purification of phenolic compounds from genipap (Genipa americana L .) extract by the ultrasound assisted ultrafiltration process. *Acta Scientiarum, 41*, 1–10. https://doi.org/10.4025/actascitechnol.v41i1.35571

Magalhães, F. de S., Sá, M. de S. M., Cardoso, V. L. & Reis, M. H. M. (2019). Recovery of phenolic compounds from pequi (Caryocar brasiliense Camb.) fruit extract by membrane filtrations: Comparison of direct and sequential processes. *Journal of Food Engineering*, *257*, 26–33. https://doi.org/10.1016/j.jfoodeng.2019.03.025

Pappas, C., Tarantilis, P. A. & Polissiou, M. (1998). Determination of Kenaf (Hibiscus cannabinus L .) Lignin in Crude Plant Material Using Diffuse Reflectance Infrared Fourier Transform Spectroscopy. *Applied Spectroscopy*, *52*(11), 1399–1402. https://doi.org/https://doi.org/10.1366/0003702981943013

Paraíso, C. M., dos Santos, S. S., Correa, V. G., Magon, T., Peralta, R. M., Visentainer, J. V. & Madrona, G. S. (2019). Ultrasound assisted extraction of hibiscus (Hibiscus sabdariffa L.) bioactive compounds for application as potential functional ingredient. *Journal of Food Science and Technology*, *56*(10), 4667–4677. https://doi.org/10.1007/s13197-019-03919-y

Paraíso, C. M., dos Santos, S. S., Pereira Bessa, L., Lopes, A. P., Ogawa, C. Y. L., da Costa, S. C., Reis, M. H. M., Filho, U. C., Sato, F., Visentainer, J. V. & Madrona, G. S. (2020). Performance of asymmetric spinel hollow fiber membranes for hibiscus (Hibiscus sabdariffa L.) extract clarification: Flux modeling and extract stability. *Journal of Food Processing and Preservation*, *44*(12), 1–13. https://doi.org/10.1111/jfpp.14948

Paraíso, C. M., Santos, S. S. dos, Ogawa, C. Y. L., Sato, F., Santos, O. A. A. dos & Madrona, G. S. (2020). Hibiscus sabdariffa L. Extract: Characterization (FTIR-ATR), Storage Stability and Food Application. *Emirates Journal of Food and Agriculture*, *32*(1), 55–61. https://doi.org/10.9755/EJFA.2020.V32.I1.2059

Patle, T. K., Shrivas, K., Kurrey, R., Upadhyay, S., Jangde, R. & Chauhan, R. (2020). Phytochemical screening and determination of phenolics and flavonoids in Dillenia pentagyna using UV–vis and FTIR spectroscopy. *Spectrochimica Acta Part A:*

Molecular and Biomolecular Spectroscopy, *242*, 118717. https://doi.org/10.1016/J.SAA.2020.118717

Pierpoint, W. S. (2004). The extraction of enzymes from plant tissues rich in phenolic compounds. *Methods in Molecular Biology*, *244*, 65–74. https://doi.org/10.1385/1-59259-655-x:65

Pinela, J., Prieto, M. A., Pereira, E., Jabeur, I., Barreiro, M. F., Barros, L. & Ferreira, I. C. F. R. (2019). Optimization of heat- and ultrasound-assisted extraction of anthocyanins from Hibiscus sabdariffa calyces for natural food colorants. *Food Chemistry*, *275*, 309–321. https://doi.org/10.1016/j.foodchem.2018.09.118

Popović, S. & Tekić, M. N. (2011). Twisted tapes as turbulence promoters in the microfiltration of milk. *Journal of Membrane Science*, *384*(1–2), 97–106. https://doi.org/10.1016/J.MEMSCI.2011.09.016

Qin, G., Lü, X., Wei, W., Li, J., Cui, R. & Hu, S. (2015). Microfiltration of kiwifruit juice and fouling mechanism using fly-ash-based ceramic membranes. *Food and Bioproducts Processing*, *96*, 278–284. https://doi.org/10.1016/j.fbp.2015.09.006

Rabelo, R. S., MacHado, M. T. C., Martínez, J. & Hubinger, M. D. (2016). Ultrasound assisted extraction and nanofiltration of phenolic compounds from artichoke solid wastes. *Journal of Food Engineering*, *178*, 170–180. https://doi.org/10.1016/J.JFOODENG.2016.01.018

Riaz, G. & Chopra, R. (2018). A review on phytochemistry and therapeutic uses of Hibiscus sabdariffa L. *Biomedicine and Pharmacotherapy*, *102*, 575–586. https://doi.org/10.1016/j.biopha.2018.03.023

Rodrigues, Leticia Misturini, Romanini, E. B., Silva, E., Pilau, E. J., da Costa, S. C. &

Madrona, G. S. (2020). Camu-camu bioactive compounds extraction by ecofriendly sequential processes (ultrasound assisted extraction and reverse osmosis). *Ultrasonics Sonochemistry*, *64*, 105017. https://doi.org/10.1016/j.ultsonch.2020.105017

Rodrigues, Letícia Misturini, Romanini, E. B., Silva, E., Pilau, E. J., Da Costa, S. C. & Madrona, G. S. (2021). Uvaia (Eugenia pyriformis Cambess) residue as a source of antioxidants: An approach to ecofriendly extraction. *LWT*, *138*, 110785. https://doi.org/10.1016/J.LWT.2020.110785

Seifzadeh, N., Ali Sahari, M., Barzegar, M., Ahmadi Gavlighi, H., Calani, L., Del Rio, D. & Galaverna, G. (2019). Evaluation of polyphenolic compounds in membrane concentrated pistachio hull extract. *Food Chemistry*, *277*, 398–406. https://doi.org/10.1016/J.FOODCHEM.2018.10.001

Singleton, V. L., & Rossi, J. A. (1965). Colorimetry of Total Phenolics with Phosphomolybdic-Phosphotungstic Acid Reagents. *American Journal of Enology and Viticulture*, 16(3), 144–158.

Socrates, G. (2001). Infrared and Raman characteristic group frequencies: Tables and Charts. John Wiley & Sons.

Sousa, L. dos S., Cabral, B. V., Madrona, G. S., Cardoso, V. L. & Reis, M. H. M. (2016). Purification of polyphenols from green tea leaves by ultrasound assisted ultrafiltration process. *Separation and Purification Technology*, *168*, 188–198. https://doi.org/10.1016/j.seppur.2016.05.029

Tahir, H. E., Xiaobo, Z., Zhihua, L., Jiyong, S., Zhai, X., Wang, S. & Mariod, A. A. (2017). Rapid prediction of phenolic compounds and antioxidant activity of Sudanese honey using Raman and Fourier transform infrared (FT-IR) spectroscopy.

Food Chemistry, *226*, 202–211. https://doi.org/10.1016/J.FOODCHEM.2017.01.024

Tsai, H. Y., Huang, A., soesanto, J. F., Luo, Y. L., Hsu, T. Y., Chen, C. H., Hwang, K. J., Ho, C. D. & Tung, K. L. (2019). 3D printing design of turbulence promoters in a cross-flow microfiltration system for fine particles removal. *Journal of Membrane Science*, *573*, 647–656. https://doi.org/10.1016/J.MEMSCI.2018.11.081

Vieira, G. S., Moreira, F. K. V., Matsumoto, R. L. S., Michelon, M., Filho, F. M. & Hubinger, M. D. (2018). Influence of nanofiltration membrane features on enrichment of jussara ethanolic extract (Euterpe edulis) in anthocyanins. *Journal of Food Engineering*, *226*, 31–41. https://doi.org/10.1016/j.jfoodeng.2018.01.013

Table 1- Coefficient of determination (R^2) for adjustment of experimental flux data to the flux decay model proposed by Field et al. (1995)

Fouling mechanism- technique	Control	Ultrasound	Turbulence promoter	Promoter+ Ultrasound
Cake formation (n = 0)	0.918	0.856	0.919	0.982
Partial pore blocking (n = 1.0)	0.992	0.980	0.983	0.991
Internal pore blocking (n = 1.5)	0.996	0.997	0.993	0.988
Complete pore blocking (n = 2.0)	0.983	0.997	0.993	0.980

Table 2- Hydraulic resistance (Membrane resistance (R_M), Cake resistance (R_C), Pore blockage resistance (R_P) and Total resistance (R_T).

Process	Resistances (10^{12} m^{-1})			
	R_M	R_C	R_P	R_T
Control	0.452	1.130	0.887	2.470
Ultrasound	0.491	1.155	0.606	2.210
Turbulence promoter	0.473	0.727	0.533	1.708
Promoter + Ultrasound	0.420	0.594	0.493	1.530

Table 3- Physicochemical analyses of hibiscus extract before and after ultrafiltration.

Membrane	Extract	Control	Promoter +Ultrassound
		Permeate	Permeate
pH	2.81^{b}±0.01	2.83^{a}±0.00	2.83^{a}±0.01
TSS (°Brix)	4.9^{a}±0,00	2.4^{b}±0,15	2.4^{b}±0,10
TS (mg/L)	52790^{a}±14.14	29030^{b}±70.71	29000^{a}±56.57
L*	19.55^{b}±0.02	33.18^{a}±0.03	33.17^{a}±0.04
a*	1.67^{b}±0,05	13.65^{a}±0,09	13.66^{a}±0,07
b*	2.25^{b}±0,09	13.70^{a}±0,03	13.68^{a}±0,06
TPC (mg EAG/g)	2.56^{a}±0,03	0.76^{b}±0,01	0.75^{b}±0,01
TA (mg C3G/100g)	295.69^{a}±2,12	11.03^{b}±0,77	12.39^{b}±2,01
Cyanidin-3-glucoside (mg/g)	0.438^{a}±0,020	0.146^{b}±0,003	0.163^{b}±0,045
Delphinidin (mg/g)	26.109^{a}±0,002	7.880^{b}±0,529	8.442^{b}±0,192
Quercetin (mg/g)	0.302^{a}±0,018	0.027^{b}±0,003	0.026^{b}±0,004
Myricetin (mg/g)	0.081^{a}±0,005	0.016^{b}±0,002	0.012^{b}±0,002
Gallic acid (mg/g)	<LQ	<LQ	<LQ
Rutin (mg/g)	0.719^{a}±0,000	0.180^{b}±0,021	0.202^{b}±0,003
p-coumaric (mg/g)	0.020^{b}±0,003	0.028^{a}±0,003	0.029^{a}±0,003
Ellagic acid (mg/g)	0.060±0,029	<LQ	<LQ
AA (mM TE/ g)	101.67^{a}±3,77	47.01^{b}±0,39	47.96^{b}±0,63

The values are the mean ± standard deviation for triplicates. Mean values denoted by a different letter along a line are significantly different at $p \leq 0.05$. LQ: Quantification limit. LD: Detection limit. Total soluble solids (TSS), total solids (TS), total phenolic compounds (TPC), total anthocyanins (TA), antioxidant activity (AA).

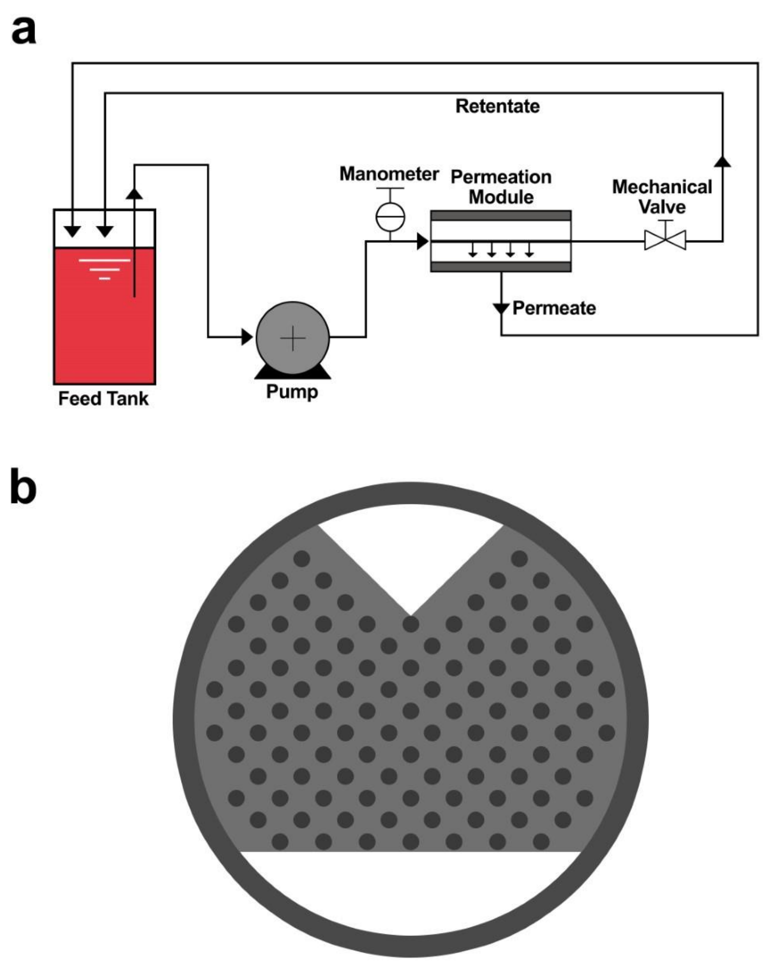

Figure 1- (A) Schematic diagram for cross-flow filtration of hibiscus extract through membranes and (B) Scheme of the projected turbulence promoter

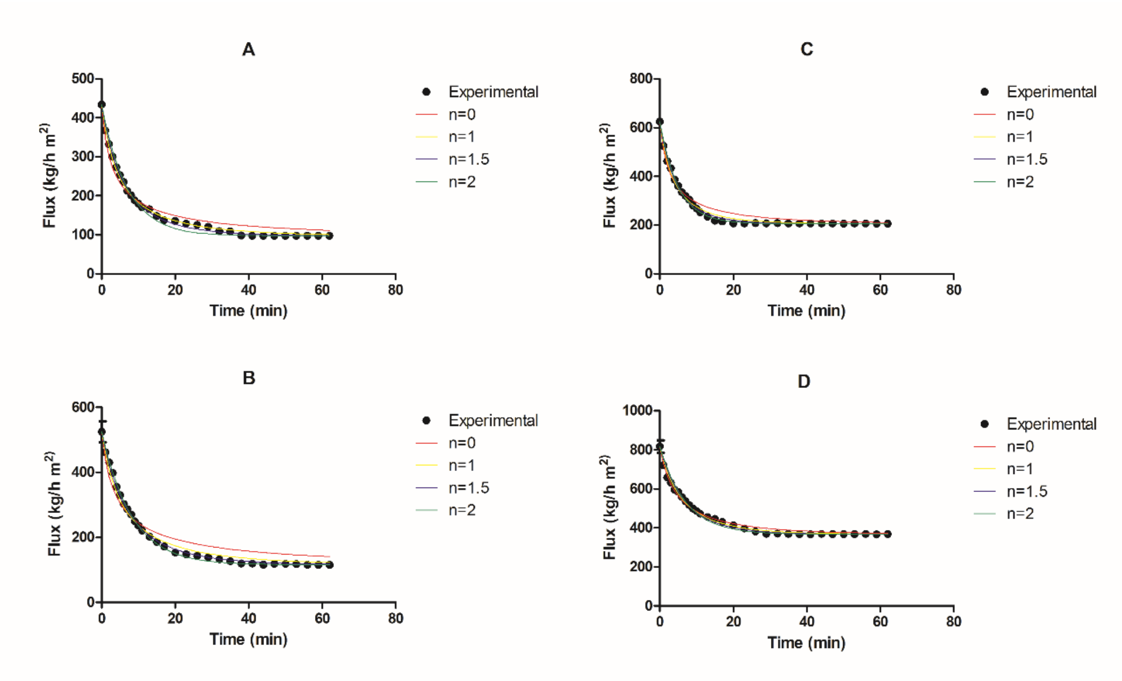

Figure 2- Experimental and calculated flux data for hibiscus extract by Field et al. (1995). Control (A), Ultrasound (B), Turbulence Promoter (C) and Promoter+Ultrasound. Cake formation (n = 0), partial pore blockage (n = 1), internal pore blockage (n = 1.5) and complete pore blockage (n = 2).

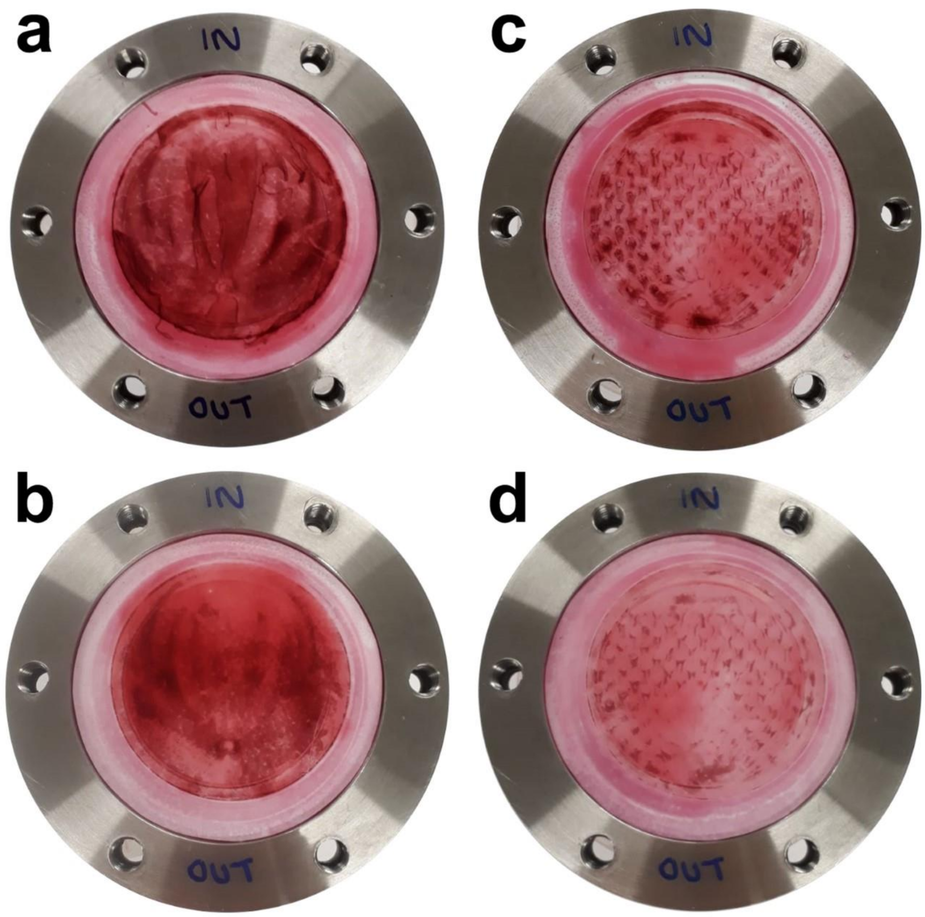

Figure 3- Visual aspect of membranes after hibiscus extract filtration. Control (A), Ultrasound (B), Turbulence Promoter (C) and Promoter+ultrasound (D).

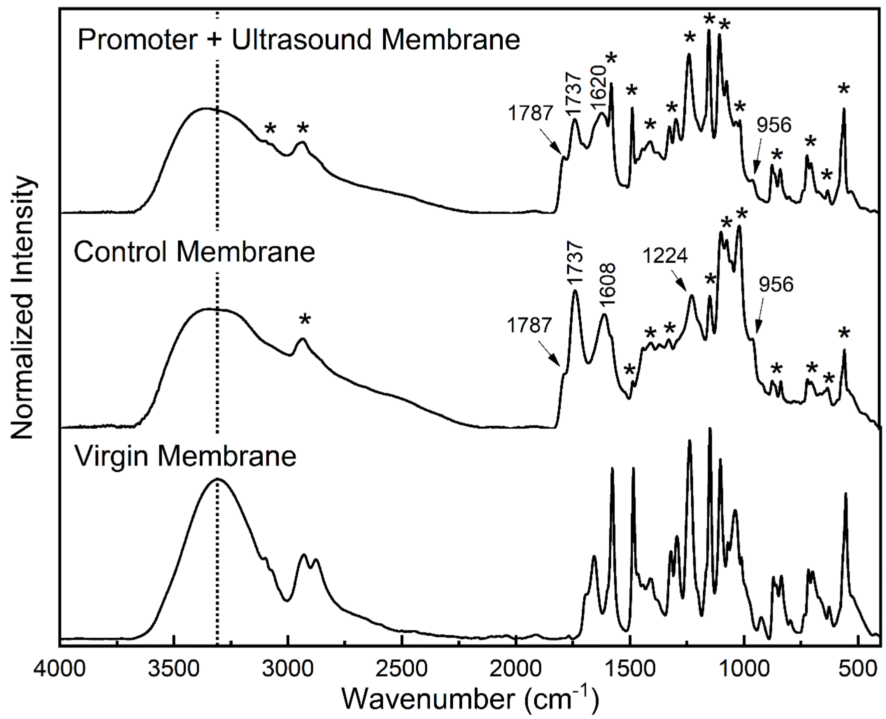

Figure 4- FTIR-ATR spectra of virgin, control, and promoter+ultrasound membrane.

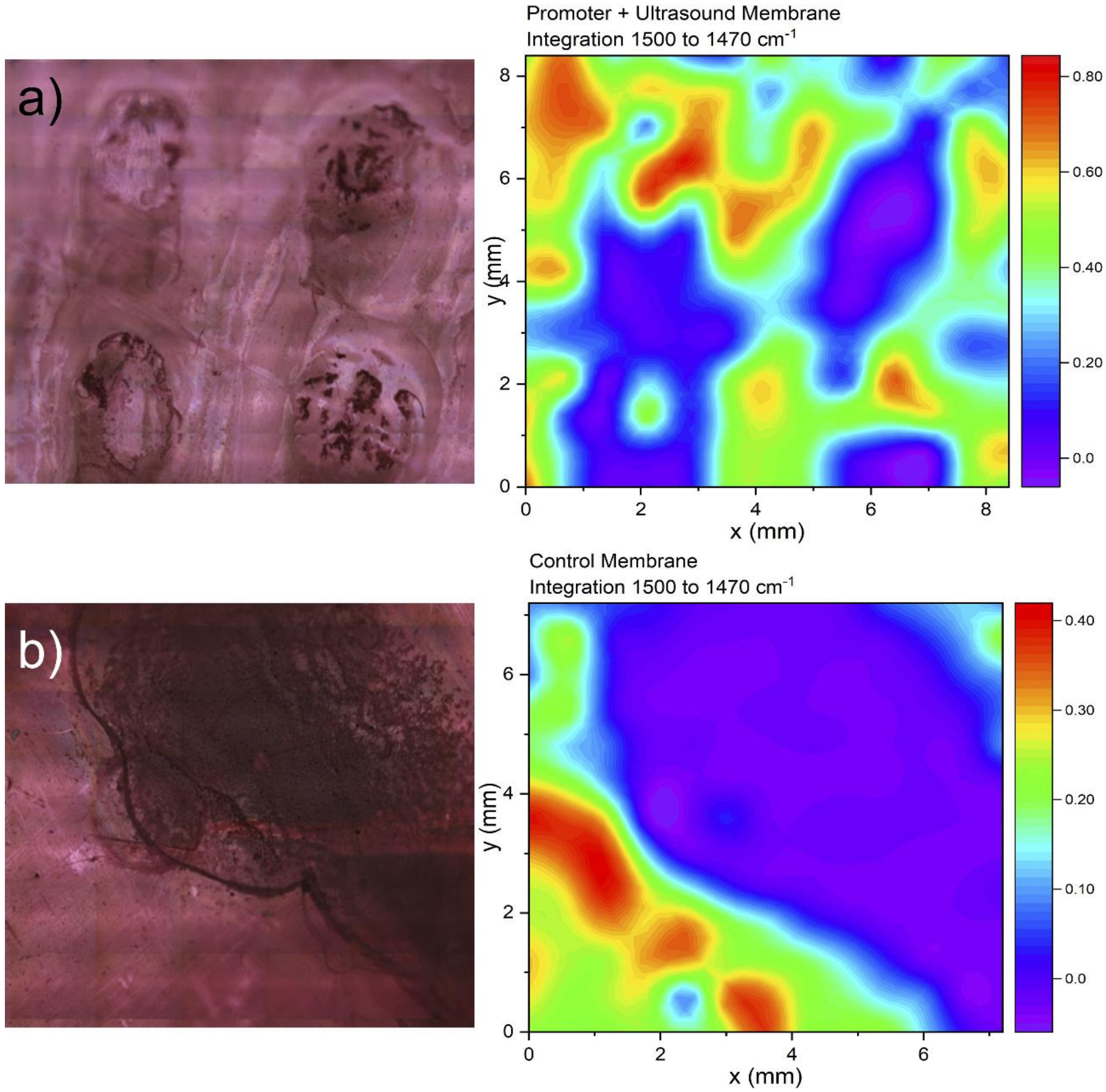

Figure 5- Surface of the promoter+ultrasound membrane (A) and control membrane and their respective maps of the area between 1500 and 1470 cm^{-1} (band associated with polyethersulfone membrane) (B).

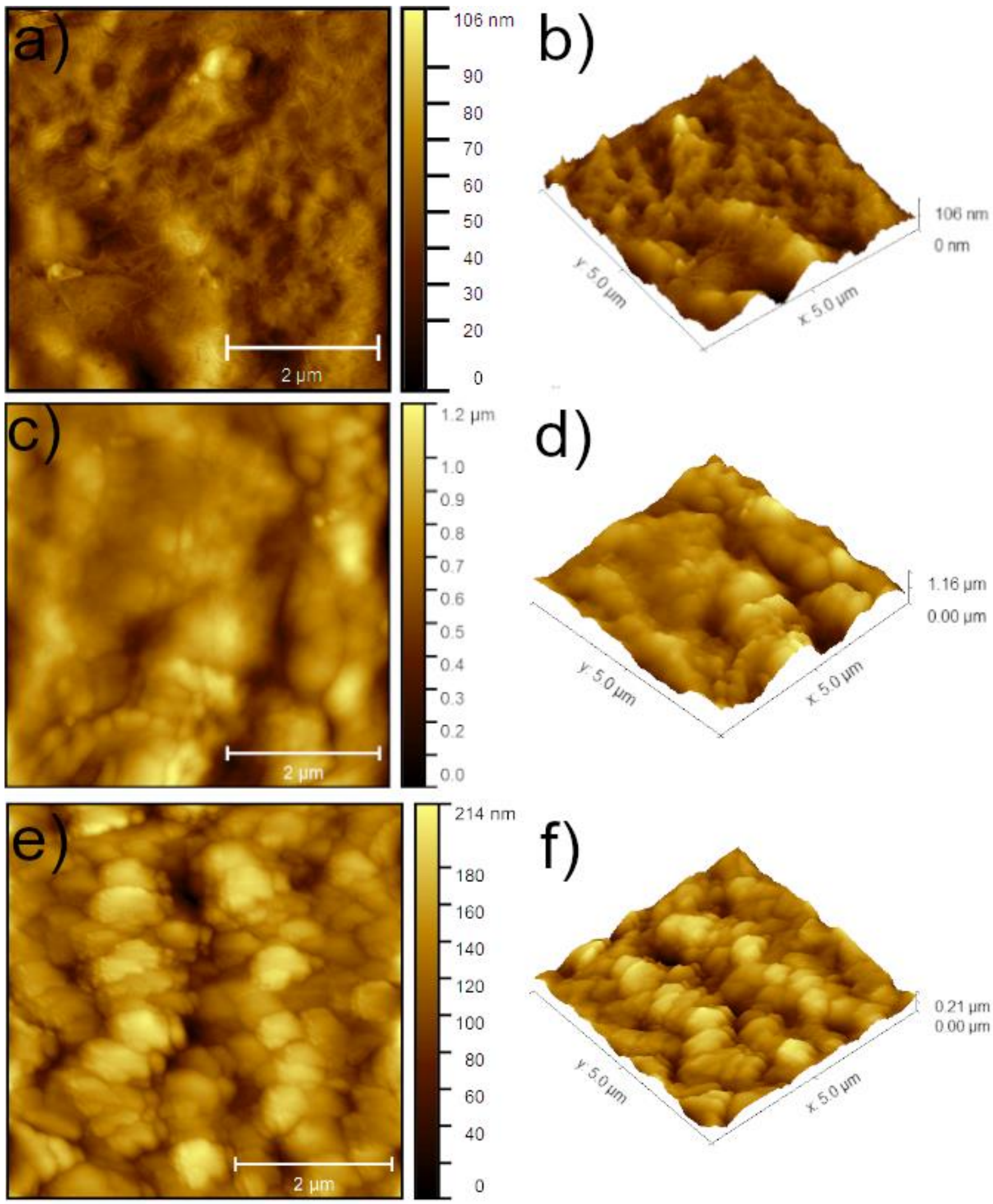

Figure 6- Morphology of membranes (A) and (B) virgin, (C) and (D) control and (E) and (F) promoter+ultrasound.

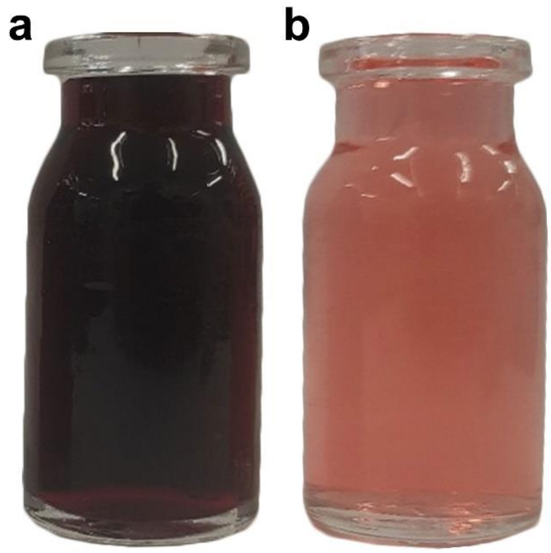

Figure 7- Visual appearance of (A) feed and (B) permeate hibiscus extracts.